EXCRESCENCE DRAG LEVELS ON AIRCRAFT

1. NOTATION AND UNITS

		SI	*British*
a	speed of sound	m/s	ft/s
b	span	m	ft
C_F	mean skin friction coefficient		
C_f	local skin friction coefficient		
D	drag	N	lbf
$f_{Hp,M}$	factor to account for variation of excrescence drag with H_p and M, see Section 6 and Appendix B		
H_p	pressure height	m	ft
h_{fin}	fin height, measured from root chord	m	ft
k	sand roughness height	m	ft
M	Mach number, V/a		
m	aircraft mass	kg	slug
q	kinetic pressure, $\rho V^2/2$	N/m^2	lbf/ft^2
S	wing reference area	m^2	ft^2
S_{wet}	aircraft wetted area	m^2	ft^2
s	fraction of semi span (or fin height) occupied by movable aerodynamic surfaces (controls, flaps, slats, spoilers)		
V	true airspeed	m/s	ft/s
W	aircraft weight	N	lbf
$\Delta[D/q]_e$	increment in (parasite) "drag area" due to excrescences	m^2	ft^2
ρ	density of air	kg/m^3	$slug/ft^3$

Subscripts

datum	denotes datum condition, i.e. H_p = 36 089 ft (11 000 m) and M = 0.8
e	denotes excrescence
fin	denotes fin
le	denotes leading edge
tail	denotes tail
te	denotes trailing edge
wing	denotes wing

2. INTRODUCTION

This Data Item gives excrescence drag data based on values for a large number of aircraft and so provides a guide to standards that have been achieved and a first approximation for estimation purposes. The term "excrescence" is defined in **Section** 3.

Most of the data are presented as values of the parameter $\Delta[D/q]_{e,\,datum}$ for the datum flight condition: H_p = 36 089 ft (11 000 m) and M = 0.8. Adjustments to other values of H_p and M are made using the method of **Section** 6 which provides values of the factor $f_{Hp,\,M}$ so that

$$\Delta\left[\frac{D}{q}\right]_e = \Delta\left[\frac{D}{q}\right]_{e,\,datum} \times f_{Hp,\,M}\,. \tag{2.1}$$

Section 4 presents values of $\Delta[D/q]_{e,\,datum}$ for complete aircraft; **Section** 5 provides an estimation method based on the breakdown of excrescence drag into various contributions. **Section** 7 provides data on the extent to which excrescence drag "clean up" has proved possible on several aircraft.

The data used in compiling Sections 4, 5 and 7 are manufacturers' estimated values for the aircraft as manufactured (and, in Section 7, as subsequently modified); **Section** 8 gives background information regarding these data. The use of estimated data is unavoidable because in most cases the drag due to an individual excrescence is not identifiable from flight-test measurements. However, Reference 8 shows how the combined effect on aircraft performance of several small airframe changes may be identified by the application of statistical principles to a set of flight-test measurements. Effects of airframe deterioration in service or of non-standard build are not considered. The effects on performance of airframe variability are considered on a statistical basis in Reference 7.

This Data Item deals only with airframe drag, but small surface features can affect both lift and moment characteristics – particularly if they influence shock wave development or boundary layer separation. In addition to influencing handling characteristics, these features can also result in noise and vibration – with implications for crew fatigue and passenger comfort. Excrescences can also affect significantly the radar cross section of an aircraft – particular examples are the presence of access panels, auxiliary intakes and drain holes or masts on surfaces liable to be "illuminated" by radar.

3. DEFINITION OF "EXCRESCENCE" FOR THIS DATA ITEM

The term excrescence *could* be used to signify "all deviations from a smooth, sealed external surface" of an aircraft. For practical reasons this definition is modified to, "anything that appears on the aircraft but is not represented on the wind-tunnel model". However, if uniformly distributed roughness (corresponding to painted, metallic or other surface finishes) is dealt with as indicated in Section 8.1.3, the definition of "excrescence" becomes, "*anything other than distributed (or "sand grain") roughness that appears on the aircraft but is not represented on a wind-tunnel model or equivalent theoretical model*". The data given in this Item are consistent with this definition. The categories of excrescences in Section 5 provide amplification of this definition while Appendix A lists individual excrescences.

The following items are **EXCLUDED** from the estimation methods of this Data Item:

Vortex generators, fences	–	but see Section 5.4,
Flap tracks, engine, stores pylons	–	treat as separate items,
Thrust reversers	–	if turning vanes are exposed, treat as separate items,
Refuelling probe	–	treat as separate item.

4. OVERALL LEVELS OF EXCRESCENCE DRAG ON COMPLETE AIRCRAFT

Figure 1 gives an approximate guide to overall excrescence drag levels for a wide range of aircraft. The characteristics of the aircraft for which data were available are summarised in Table 8.1. Where possible, the data have been adjusted to accord with the definition of Section 3, for example by the deletion of components that are excluded there. No further attempt has been made to allow for differences between what constitute excrescences for the various manufacturers concerned. Greater certainty as to *what* excrescences are included can be obtained by using the method of Section 5.

5. CONTRIBUTIONS TO EXCRESCENCE DRAG ON AIRCRAFT

Figures 2 to 7 give values of contributions to $\Delta[D/q]_{e,datum}$ for the following categories of excrescence.

Category of excrescence			see Section	see Figure	see Appendix A Section
Basic airframe	1.	Airframe-build surface imperfections.	5.1	2	A1
	2.	Imperfections associated with movable aerodynamic surfaces.	5.1	3	A2
Fixed external components of aircraft systems	3.	Air data sensors.	5.2	4(a)	A3
	4.	Lights and beacons.	5.2	4(b)	A4.
	5.	Antennae.	5.2	4(c)	A5
	6.	Static discharge wicks.	5.2	4(d)	A6
	7.	Rain dispersal: screen wipers/blowing/fluid; gutters over doors.	5.2	4(e)	A7
	8.	Drains.	5.2	4(f)	A8
	9.	Fuel system.	5.2	4(g)	A9
Internal Airflow Systems	10.	Ventilation/cooling.	5.3	5	A10.
	11.	Air conditioning/pressurisation.	5.3	6	A11
	12.	Auxiliary power unit.	5.3	7	A12
	13.	Miscellaneous airframe features.	5.4	–	–

Appendix A gives a detailed listing of excrescences included in the categories identified in the above Table. The categories are close to those used for several aircraft for which data were available but are chosen to take maximum advantage of data for a wider range of aircraft where no common set of categories has been used. The inclusion in the list of several very small items is justified by the possibility that for some classes of aircraft one or more of such items may not be present.

Table 8.2 describes the aircraft for which detailed excrescence drag data were available.

5.1 Excrescence Drag Associated with Basic Airframe (Categories 1, 2)

Figures 2 and 3 give data, respectively, for airframe-build surface imperfections and for imperfections associated with movable aerodynamic surfaces. These are the most numerous sources of excrescence drag and are directly related to the standards of airframe design and construction. Drag improvements in these categories can be very significant but are likely to take much time, effort and expense to achieve. The quantity of data available was greatest in these Categories but the standards of construction represented are correspondingly wide.

In Figure 3 the independent variable is the parameter

$$b_{wing}[s_{le}+s_{te}]_{wing} + b_{tail}\,s_{te_{tail}} + h_{fin}\,s_{te_{fin}}.$$

The spanwise fractions, s, are evaluated for all slots, steps and gaps for each relevant surface, *e.g.* control, slat, flap, spoiler.

5.2 Excrescence Drag Due to Fixed External Components of Aircraft Systems (Categories 3 to 9)

These Categories cover the bulk of external features not associated with the basic airframe. Some are relatively large – at least as compared with typical boundary layer thicknesses.

Air Data Sensors, Figure 4(a): The data apply to typical installations of pitot, pitot-static, static pressure sensors, outside air temperature sensors and flow direction sensors.

Lights and Beacons, Figure 4(b): Anti-collision beacons predominate on current aircraft; navigation lights are generally flush and give little drag. Landing lights are not considered; they are usually flush mounted in a forward facing surface or mounted on the undercarriage.

Antennae, Figure 4(c): The following trends are illustrated:

(i) improved antenna design can reduce drag dramatically,
(ii) higher maximum speeds necessitate lower-drag installations,
(iii) an empirical, but fairly consistent, increase in drag with range.

Static Discharge Wicks, Figure 4(d): The data apply to modern, rigid static discharge wicks; older, flexible types tend to be larger but no data are available. Static wicks are located on the relatively-sharp tip and trailing surfaces of the airframe, primarily to avoid intermittent and sudden electric discharges which can interfere with electronic and communications equipment. Advantages in terms of safety (*e.g.* at refuelling) and comfort (*e.g.* at unloading) are recognised but many aircraft have no static wicks. The mechanism of static electricity generation is friction and so airframe wetted area might seem a relevant parameter. The use of frontal area in the figure was suggested by a manufacturer and found advantageous.

Rain Dispersal, Figure 4(e): A wide range of drag values is quoted for screen wipers. The "low drag dispersal systems" in the Figure include both low drag and/or faired wipers and cases where dispersal is accomplished by air blast from nozzles (contributions due to screen washers are included in the quoted values). The installation of screen wipers or air blast systems is part of a larger (certification) issue of pilot clear vision which includes the effects of rain, snow, ice and other contaminants and debris, *e.g.* following a bird strike. Other factors include the provision of clear-view (openable) panels, screen washers, water repellent coatings and screen geometry, especially sweep angles. Most large transport-category aircraft are equipped with screen wipers; air-blast systems can be used but equivalent performance is required. On some smaller transport types, certification may be possible without either wipers or air blast systems. Most combat aircraft have some form of screen clearance system; air-blast systems are often used.

Drains, Figure 4(f): This encompasses all forms of masts and holes for rain, fuel, oil and other fluids. The relevant components from the systems considered in Section 5.3 are included. The use of aircraft maximum weight as the independent variable in Figure 4(f) implies only that no other relevant parameter has been identified.

Fuel System, Figure 4(g): This category does not include drag due to fuel tank access panels – which often occur in large numbers on the wing lower surface (and occasionally on upper surfaces). It was convenient to include the drag due to such panels in Category 1 because this involved the least adjustment of the available data.

5.3 Excrescence Drag Associated with Internal Airflow Systems (Categories 10, 11, 12)

Ventilation/cooling, air conditioning and auxiliary power unit systems involve inlets and outlets/exhausts in the airframe surface – not all of which will be in use during all (or even any) flight phases. These categories have proved to be the most difficult to generalise. The values quoted apply to the en-route or cruise configuration and include, where appropriate, system internal momentum losses. Much depends on the location and forms of the inlets and outlets and on whether either (particularly inlets) can be sealed when not in use.

The following paragraphs treat Categories 10, 11, 12 separately. However, the distinction between ventilation/cooling and air conditioning is by no means the same on all aircraft. Whatever the precise sub-division of these functions may be in a particular aircraft, it is suggested that contributions from categories 10 and 11 should be included in any overall estimate.

Ventilation/Cooling, Figure 5: These terms imply the exposure of airframe, engine and systems components to atmosphere air conditions. This may be achieved passively using ventilation holes, grills *etc*, or by the use of dedicated scoop or flush inlets (with or without power assistance) or as part of larger systems such as the (boundary layer) bleeds and (engine) bypass or spill airflows on many high performance aircraft.

Cooling Airflows for piston engines are *not* included – whether the engine is “air” or “liquid” cooled. This is a major drag component in its own right and should be treated as such. No data are included in Figure 5 for aircraft with turbo-prop engines.

Air Conditioning/Pressurisation, Figure 6: The term implies a system providing large quantities of air at conditions of temperature, pressure and humidity which may be far removed from ambient. In most modern systems this air is bled initially from one or more stages of the engine compressor and subsequently “conditioned” by passage through heat exchanger and water separator and injector stages.

The primary effect of compressor air bleed on performance is taken into account as a loss of engine thrust (or power). Subsequent thrust recovery from the exhausting of cabin air is considered here as a negative contribution to excrescence drag. Maximum achieved values of thrust recovery are quoted but these imply the provision of suitable exhaust vents and a well-sealed fuselage. The other major direct effect of the air conditioning system is the drag ascribed to leakage where the fuselage is not sealed. Figure 6 quotes only maximum values.

The remaining effects on excrescence drag arise from pressure relief valves and the inlets and outlets for the cooling air used in the system heat exchangers and similar comments apply to those mentioned under "Ventilation/cooling".

Auxiliary Power Unit, Figure 7: The main functions are, typically, to provide

compressed air for the air conditioning system when on the ground,
compressed air for main engine start up,
shaft power for ground or emergency in-flight electrical power generation.

In many cases all three functions apply but for the purpose of this Data Item it has been found useful to consider only the air bleed capabilities of the unit.

Excrescence drag arises primarily due to the inlet and exhaust systems. On some installations the inlet(s) can be blanked off or retracted so that only the exhaust contributes to drag. If the exhaust is located in a rearward facing surface – usually the fuselage tailcone – its presence will not change whatever base drag has already been allowed. If a unit is to be used in flight it may be necessary to remove (divert) the airframe boundary layer ahead of the inlet – with an attendent drag penalty. This is particularly important if a unit is certificated to provide in-flight electrical power and/or bleed air when one of the main engines is inoperative.

5.4 Miscellaneous Drag Producing Features

Many aircraft carry features that do not fit easily into Categories 1 to 12. Alternatively, while a feature might fit into one of the categories, its occurrence might be so infrequent as to make its inclusion in that category of no practical value. This final Category presents some of the limited available data while adhering as closely as possible to the definition in Section 3.

Vortex generators: The flight conditions at which aircraft can operate are frequently constrained by the effects of boundary layer separation. Vortex generators provide an effective means of alleviating these effects while entailing only minor changes to the airframe.

In flow conditions where vortex generators are required to be effective, there may be an overall reduction in the drag of the airframe component on which they are installed – due to the separation control they provide. In such cases they should not be regarded as excrescences but as part of the basic wing, *etc*. For flow conditions where the vortex generators are not required to control separation (and these could include normal cruise conditions), information given in References 21 and 22 may be used to predict the "direct" drag of vane vortex generators. Section 8.1.1 of Reference 21 describes the estimation procedure in detail but the data of Reference 22 alone can be used to estimate the drag contribution due to a single vane, of height h_v, as

$$\left[\frac{\Delta D}{q}\right]_e = \frac{\frac{1}{2}\rho_v U_v^2}{q} h_v^2 [k_D \cos\sigma \pm k_v \sin\sigma] \ . \qquad (5.1)$$

k_D, k_v: vane drag and vortex strength (lift) parameters, relative to local flow direction; Figure 2 of Reference 22 gives values as function of planform and incidence.

U_v, ρ_v: velocity and density at edge of boundary layer at vane location.

σ: angle between freestream and flow at vane; Figure 4 of Reference 22 gives values.

Gun installation: For a single barrel gun (20 mm or 30 mm) installed within the fuselage

$$\Delta[D/q]_{e,\,datum} = 0.03 \text{ to } 0.04 \text{ ft}^2 . \tag{5.2}$$

This includes the drag due to the "break out" in the fuselage surface and an allowance for inlet/outlet of purging air and holes for the ejection of spent cartridges.

Arrester hook: Depending on the hook size and installation, values lie in the range

$$\Delta[D/q]_{e,\,datum} = 0.025 \text{ to } 0.1 \text{ ft}^2 . \tag{5.3}$$

Open holes with transverse vanes (or cascades): Some exhausts (including some older-style thrust-reverser outlets) take this form and the limited data available suggest that

$$\Delta[D/q]_{e,\,datum} = 0.075 + 0.25 \times 10^{-3} \left[\begin{array}{l} \text{design airflow through} \\ \text{hole, in lbf/s} \end{array} \right] \text{ft}^2 . \tag{5.4}$$

6. EFFECT OF CHANGES IN H_p AND M ON EXCRESCENCE DRAG

Figure 8 gives an approximate method for adjusting the *summation* of the values of $\Delta[D/q]_{e,\,datum}$ obtained from Figures 1 to 7, (and applicable to H_p = 36 089 ft (11 000 m) and M = 0.8) to other combinations of H_p and M. These data are deduced from the typical variation with Mach and Reynolds numbers of drag data for excrescences where the mean height is of the order 0.1 of the boundary layer thickness. While this approach is clearly incorrect for relatively large excrescences such as antennae or air data sensors, it is acceptable when applied to the overall level of excrescence drag on an aircraft because of the relatively small average height of excrescences. In Figure 8 values are given of the parameter $f_{H_{p,\,M}}$, where

$$f_{H_{p,\,M}} = \frac{\Delta[D/q]_e}{\Delta[D/q]_{e,\,datum}}, \tag{6.1}$$

and $\Delta[D/q]_{e,\,datum}$ is the datum value, estimated using Sections 4 or 5, for H_p = 36 089 ft and M = 0.8. The Figure includes data for three forms of excrescence, as follows

(a) aft facing steps,
(b) forward facing steps,
(c) grooves transverse to flow.

A value of $f_{H_{p,\,M}}$ can be assessed as some combination of the values given in Figures 8(a) to 8(c). It is recommended that,

for conservative results, use Figure 8(a) (aft facing steps),
for typical airframe, use average of values from Figures 8(a) and 8(b),
use Figure 8(c) only in circumstances where it is obviously relevant.

Appendix B gives a derivation of the relationships presented in Figure 8.

7. EXCRESCENCE DRAG CLEAN-UP

The level of excrescence drag on an airframe is, at least in principle, optional – although much detail-design effort is required if a low excrescence drag is to be achieved. Figure 9 shows examples of the extent to which airframe "clean-up" has reduced the level of excrescence drag between different versions of particular aircraft types. The examples include

changes between prototype and initial production standard,
changes between early production standard and improved standard,
changes between "basic" aircraft and a derivative thereof.

Information regarding time, cost and effort required to bring about these improvements is not available although the times range between one and ten years for the extreme cases.

8. NOTES ON DATA USED IN PREPARING THIS DATA ITEM

In preparing this Data Item a large number of diverse topics has been considered and many of these are addressed in Section 5 and Appendices A and B. This Section deals with two areas that remain. Section 8.1 summarises the methods used to treat several aerodynamic phenomena so as to distinguish them (by implication, at least) from "excrescence drag" as treated here. Section 8.2 summarises the methods likely to have been used in generating the aircraft excresence drag data upon which Figures 1 to 9 are based. It also provides a guide to the types of aircraft for which data were available.

8.1 Distinctions Between Treatments of Skin Friction, Surface Roughness and Excrescences

8.1.1 Skin friction on smooth flat plate

In viscous flow over a smooth flat plate, skin friction arises from the shear stress at the fluid/surface interface and is represented as either a local skin friction coefficient, C_f, or a mean skin friction coefficient, C_F. The latter of these represents an integration of values of the former over the relevant streamwise distance. References 3 and 4 give data for laminar and turbulent boundary layers. Appendix B gives equations for C_f and C_F for a turbulent boundary layer.

8.1.2 Effect of surface roughness and waviness on transition

Boundary layer transition from laminar to turbulent flow is affected by the presence of surface roughness. References 1 and 2 give estimates of roughness height (uniformly distributed or discrete), and of surface waviness, below which laminar flow boundary layer development, transition position (and hence drag) are unaffected.

8.1.3 Skin friction on uniformly rough flat plate

Values of skin friction coefficient for a turbulent boundary layer on a uniformly rough flat plate can be estimated using Reference 5 which follows the widely-used practice of characterising a uniform surface roughness by an *equivalent sand roughness height, k*, – defined as the value of *k* required to produce the same mean skin friction coefficient as the actual roughness.

8.1.4 Non-uniformly distributed roughness

Non-uniformly distributed roughness may also be represented by an equivalent sand roughness height – *i.e* as the value of *k* required, for uniform surface roughess, to produce the same mean skin friction as the actual, non-uniform, roughness. This concept has been used to characterise excrescence drag levels on some aircraft. **Excrescence drag is not represented in this way in this Data Item**.

8.1.5 Drag due to individual excrescences

For a laminar boundary layer, if an excrescence is so small as to have no effect on transition, it can have only negligible effect on drag. If an excrescence is of sufficient height to influence transition of a laminar boundary layer (see Reference 2), increased drag will result due to higher skin friction levels associated with a turbulent boundary layer (References 4 and 5).

References 9 to 16 give drag values for particular types of excrescence, mounted on a flat plate (zero streamwise pressure gradient) and immersed in a turbulent boundary layer. These drag values are converted to values appropriate to airframe components in the presence of finite pressure gradients by use of an excrescence drag magnification factor, see References 17 and 18.

8.2 Excrescence Drag Data for Complete Aircraft

A full estimate of excrescence drag for a complete aircraft requires a survey of the airframe and individual estimates for each excrescence (or a representative selection) using techniques such as those described in Section 8.1.5, including the use of appropriate magnification factors to account for the effects of surface pressure gradients. Examples of part of this process are given in Reference 20. Figures 1 to 7 and 9 are based on the results of detailed estimates made by aircraft manufacturers or others. It is likely that those estimates have been made with the assumption that boundary layer transition occurs well forward on each major airframe component. Figure 1 is based on overall excrescence drag values for a wide range of aircraft types and the relevant characteristics are summarised in Table 8.1. The aircraft for which detailed breakdowns of the excrescence drag values were available for Figures 2 to 7 and 9 are described in Table 8.2.

In most of these instances the data have been generated as part of thrust and drag accounting. This implies that, whatever the degree of sophistication of the methods used to estimate the excrescence drag, the results were acceptable within the overall context of reconciling flight-test measured drag with predicted values (including use of wind tunnel data, where available). The quality of the estimation of excrescence drag doubtless varies widely and it is likely to be greatest for the more modern classes of aircraft – particularly those, such as large jet transports, where the operational penalties of excessive drag can be severe.

TABLE 8.1

Class of aircraft	Number of aircraft types	Ranges of values of	
		S_{wet} ft^2	S ft^2
Jet- or fan-engined transports/bombers	36	3340 to 33000	550 to 6200
Small jet- or fan-engined transports	3	1350 to 1700	230 to 350
Propeller-driven transports	5	3500 to 13800	370 to 2500
Propeller-driven light/trainer types	2	620 and 830	150 and 210
Jet-engined combat types	51	120 to 3300	12 to 600
Piston-engined combat aircraft	55	750 to 7300	200 to 1700

TABLE 8.2

Class of aircraft	Number of aircraft types	Ranges of values of	
		S_{wet} ft^2	S ft^2
Jet- or fan-engined transports/bombers	15 (6)*	6850 to 33000 (3340 to 8000)*	1300 to 6200 (550 to 2400)*
Small jet- or fan-engined transports	1	1700	350
Propeller-driven transports	(3)*	(4250 and 7200)*	(880 to 1460)*
Propeller-driven light/trainer types	2	620 and 830	150 and 210
Jet-engined combat types	11 (16)*	900 to 2200 (540 to 1900)*	200 to 510 (120 to 780)*
Piston-engined combat aircraft	4 (51)*	790 to 5200 (750 to 7300)*	240 to 1260 (200 to 1700)*

* Older aircraft with data for only a few categories of excrescence.

9. REFERENCES

9.1 ESDU Data Items, General

1. ESDU — Limit of surface waviness for laminar flow over wings. ESDU **Aerodynamics** Data Item No. Wings 02.04.11, November 1943 (with Amendments A and B, December 1974).

2. ESDU — Limit of grain size for laminar flow over wings or bodies. ESDU **Aerodynamics** Data Item No. Wings 02.04.09, April 1953 (with Amendments A and B, July 1973).

3. ESDU — The compressible two-dimensional laminar boundary layer, both with and without heat transfer, on a smooth flat plate, with application to wedges, cylinders and cones. ESDU **Aerodynamics** Data Item No. 68019, December 1968 (with Amendments A and B, July 1973).

4. ESDU — The compressible two-dimensional turbulent boundary layer, both with and without heat transfer, on a smooth flat plate, with application to wedges, cylinders and cones. ESDU **Aerodynamics** Data Item No. 68020, May 1968 (with Amendments A to C, March 1988).

5. ESDU — The mean skin friction coefficient for a rough flat plate with a turbulent two-dimensional boundary layer in compressible adiabatic flow, with application to wedges, cylinders and cones. ESDU **Aerodynamics** Data Item No. 73016, July 1973.

6. ESDU — Equations for calculation of International Standard Atmosphere and associated off-standard atmospheres. ESDU Data Item No. 77022, November 1977 (with Amendments A and B, February 1986).

7. ESDU — Variability of standard aircraft performance parameters. ESDU Data Item No. 91020, October 1991.

8. ESDU — Example of statistical techniques applied to analysis of effects of small changes. ESDU Data Item No. 93023, November 1993.

9.2 ESDU Data Items on Excrescence Drag

9. ESDU — Approximate wave drag of rectangular planform fairings at zero incidence in supersonic flow. ESDU **Aerodynamics** Data Item No. 71018, September 1971.

10. ESDU — Drag due to a circular cavity in a plate with a turbulent boundary layer at subsonic, transonic and supersonic speeds. ESDU **Aerodynamics** Data Item No. 74036, November 1974 (with Amendment B, June 1987).

11. ESDU — Drag due to grooves in a flat plate with a turbulent boundary layer at subsonic and supersonic speeds. ESDU **Aerodynamics** Data Item No. **75028**, November 1975.

12. ESDU — Drag of **two-dimensional steps and ridges** immersed in a turbulent boundary layer for Mach numbers up to 3. ESDU **Aerodynamics** Data Item No. **75031**, November 1975 (with Amendment A, June 1987).

13. ESDU — Drag of transverse rows of spherically-headed rivets immersed in a turbulent boundary layer at subsonic and supersonic speeds. ESDU **Aerodynamics** Data Item No. 76008, April 1976.

14. ESDU — Drag of circular cylinders normal to a flat plate with a turbulent boundary layer for Mach numbers up to 3. ESDU **Aerodynamics** Data Item No. 83025, August 1983.

15. ESDU — Drag of stub wings and fairings on a flat plate with a turbulent boundary layer at subsonic and supersonic speeds. ESDU **Aerodynamics** Data Item No. 84035, November 1984 (with Amendment A, March 1988).

16. ESDU — Drag and pressure recovery characteristics of auxiliary air inlets at subsonic speeds. ESDU **Aerodynamics** Data Item No. 86002, April 1986 (with Amendment A, June 1983).

17. ESDU — Calculation of excrescence drag magnification due to pressure gradients at high subsonic speeds. ESDU **Transonic Aerodynamics** Data Item No. 87004, August 1987 (with Amendment A, November 1989).

18. ESDU — Simplified method for the prediction of aerofoil excrescence drag magnification factor for turbulent boundary layers at subcritical Mach numbers. ESDU **Aerodynamics** Data Item No. 91028, October 1991.

19. ESDU — Drag due to gaps round undeflected trailing-edge controls and flaps at subsonic speeds. ESDU **Aerodynamics** Data Item No. 92039, November 1992.

20. ESDU — Examples of excrescence drag prediction for typical wing components on a subsonic transport aircraft at the cruise condition. ESDU **Aerodynamics** Data Item No. 93032, December 1993.

21. ESDU — Vortex generators for control of shock-induced separation, part 1: introduction and aerodynamics. ESDU **Transonic Aerodynamics**, Data Item No. 93024, December 1993.

22. ESDU — Vortex generators for control of shock-induced separation, part 2: guide to use of vane vortex generators. ESDU **Transonic Aerodynamics** Data Item No. 93025, June 1994.

9.3 Other References

23. GAUDET, L. JOHNSON, P. — Measurements of the drag of various two-dimensional excrescences immersed in turbulent boundary layers at Mach numbers between 0.2 and 2.8. RAE tech. Rep. 70190, 1970.

24. SIMPER, J.I. HUTTON, P.G. — Formulae and proposed layout of graphs for the application of RAE 8 ft × 8 ft tunnel results to the rapid estimation of excrescence drag. ARA Memor. 133, 1972.

25. GAUDET, L. WINTER, K.G. — Turbulent boundary-layer studies at high Reynolds numbers at Mach numbers between 0.2 and 2.8. ARC R & M 3712, 1973.

26. PALLISTER, K.C. — Wind-tunnel measurements on the transonic drag of excrescences immersed in a turbulent boundary layer. ARA Rep. 37, 1974.

27. SOMMER, S.C. SHORT, B.J. — Free-flight measurements of turbulent boundary layer skin friction in the presence of severe aerodynamic heating at Mach numbers from 2.8 to 7. NACA Tech. Note 3391, 1955.

28. COLES, D.E. — The turbulent boundary layer in a compressible fluid. Rand Report R-403-PR, September 1962.

29. SPALDING, D.B. CHI, S.W. — The drag of a compressible turbulent boundary layer on a smooth plate with and without heat transfer. *Journal of Fluid Mechanics*, January 1964.

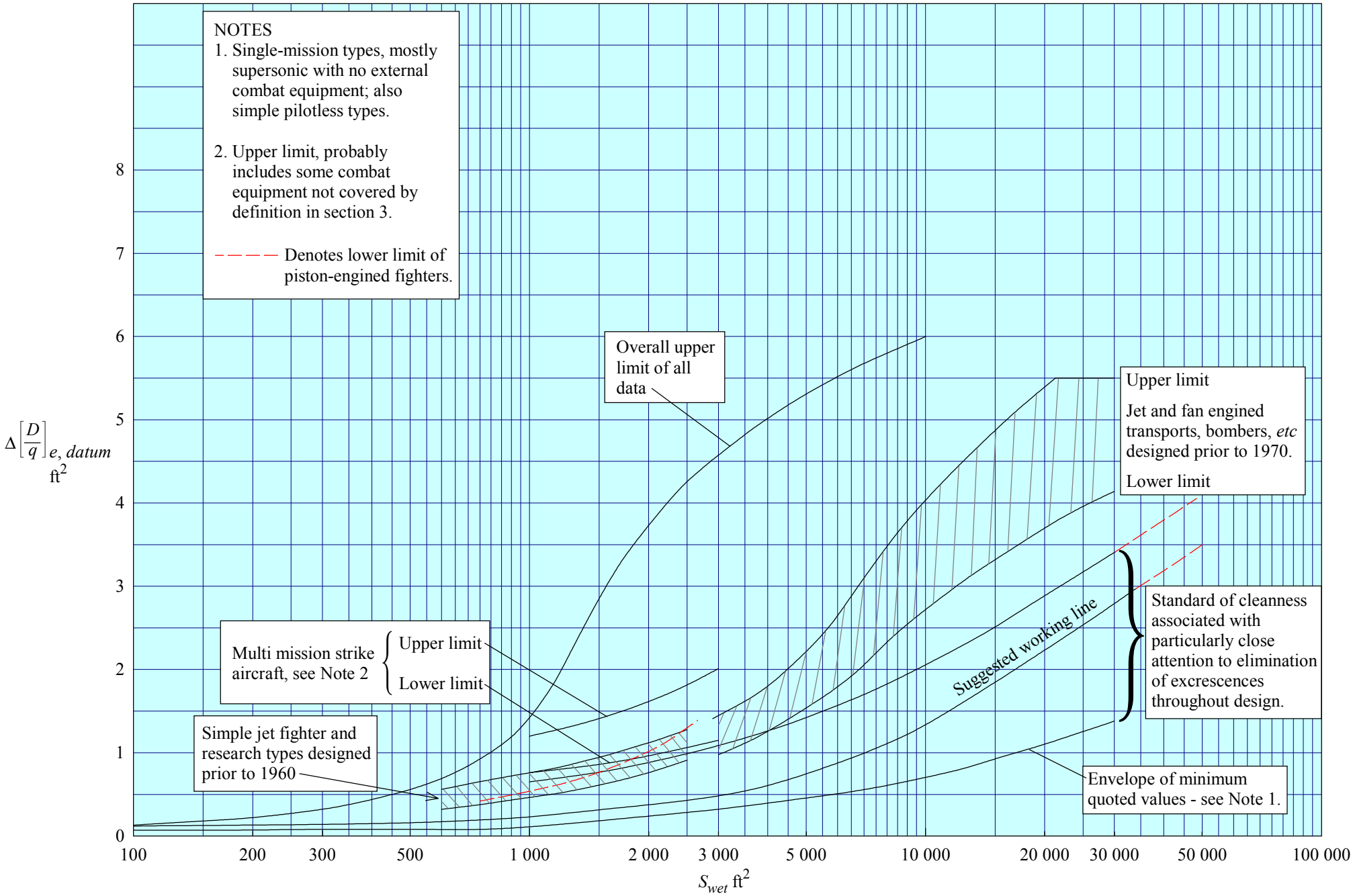

FIGURE 1 OVERALL EXCRESCENCE DRAG LEVELS ON AIRCRAFT (AT DATUM CONDITIONS OF H_p AND M)

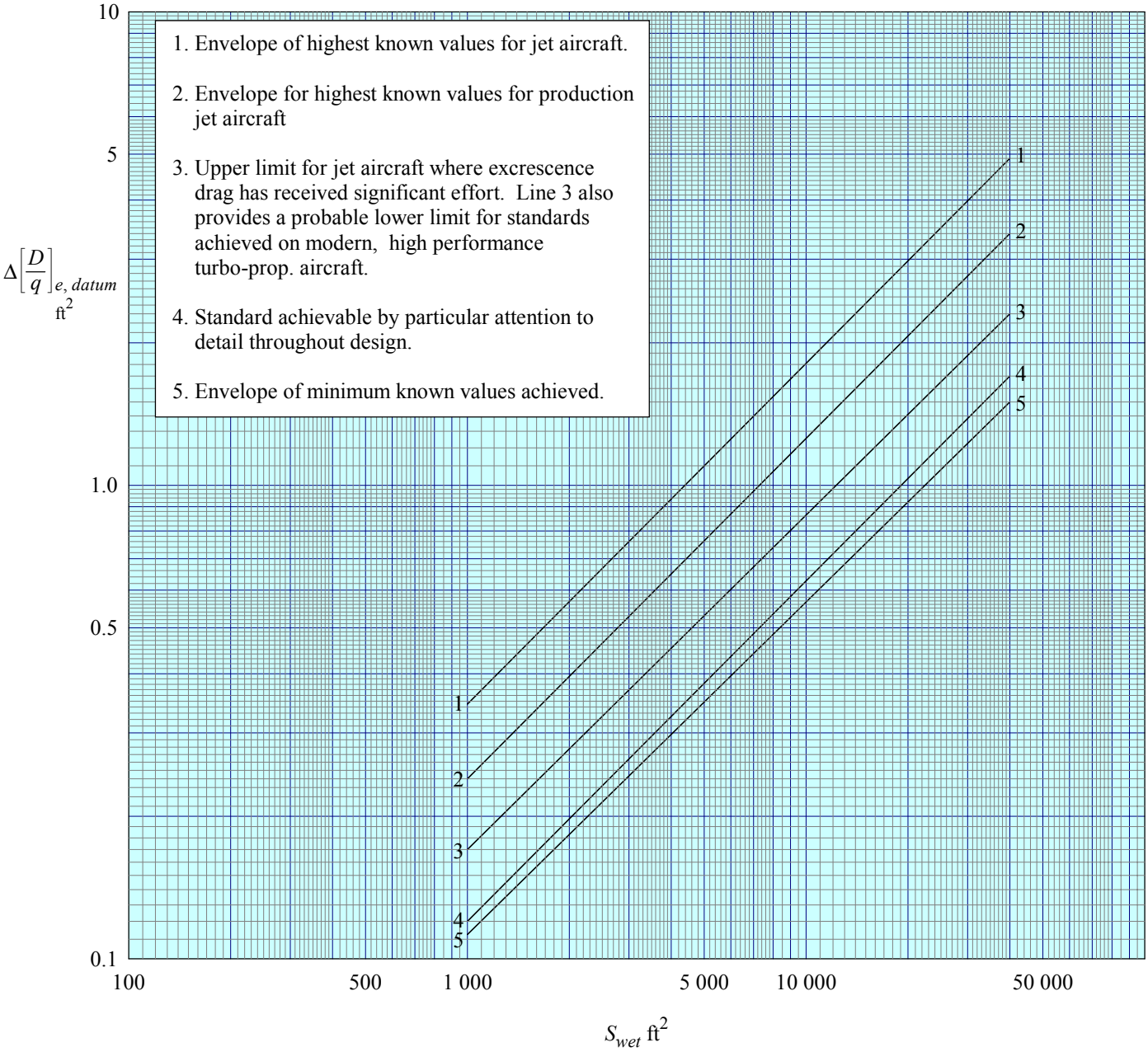

FIGURE 2 EXCRESCENCE DRAG LEVELS DUE TO AIRFRAME-BUILD SURFACE IMPERFECTIONS (AT DATUM CONDITIONS OF H_p AND M)

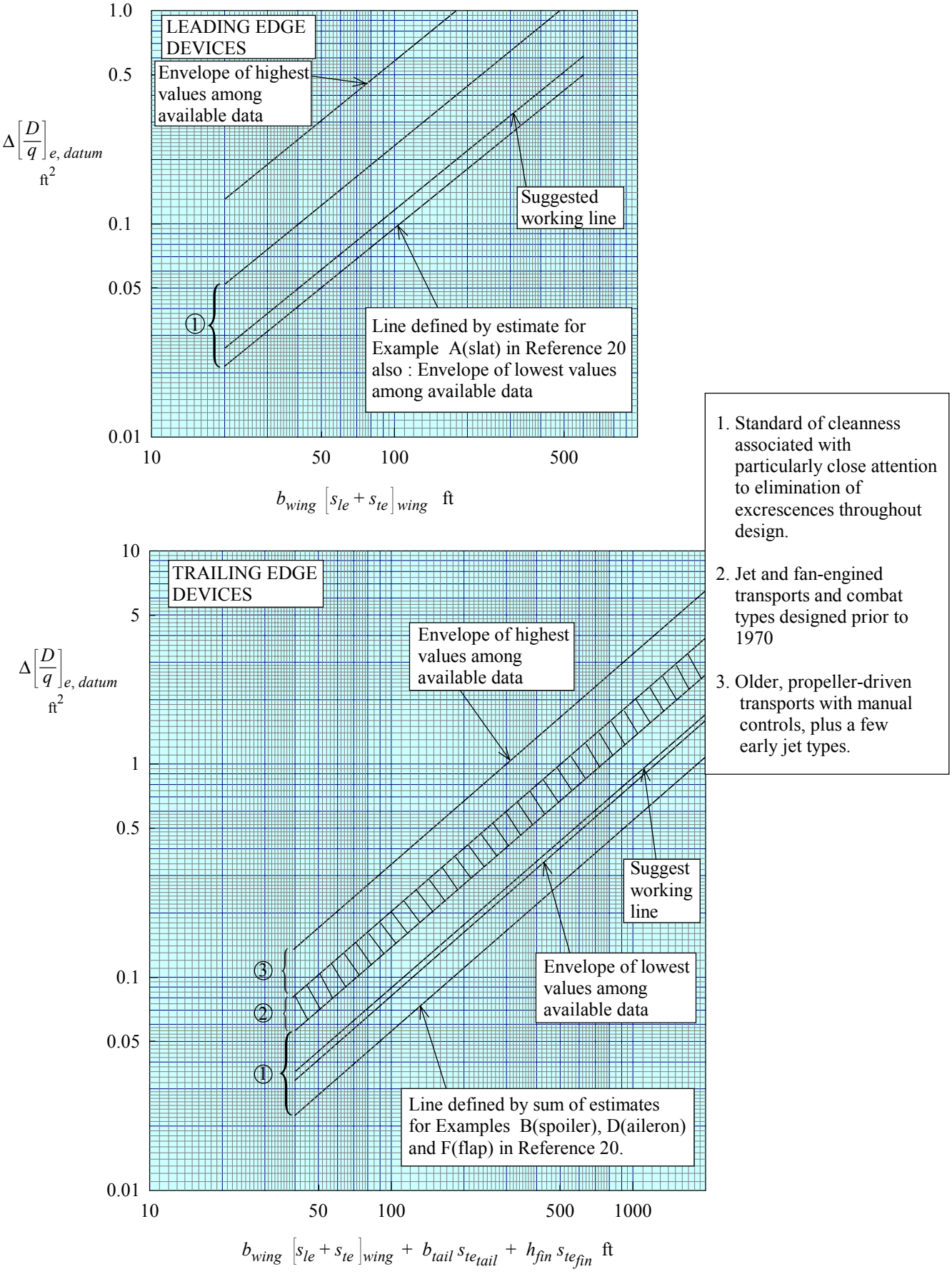

FIGURE 3 EXCRESCENCE DRAG LEVELS DUE TO IMPERFECTIONS ASSOCIATED WITH MOVABLE AERODYNAMIC SURFACES (AT DATUM CONDITIONS OF H_p AND M)

(a) AIR DATA SYSTEMS (NON-FLUSH SENSORS)

For most applications

$$\Delta\left[\frac{D}{q}\right]_{e,\ datum} = 0.02 \text{ to } 0.05 \text{ ft}^2$$

but values as high as 0.08 possible where flow direction sensors are a particular feature.

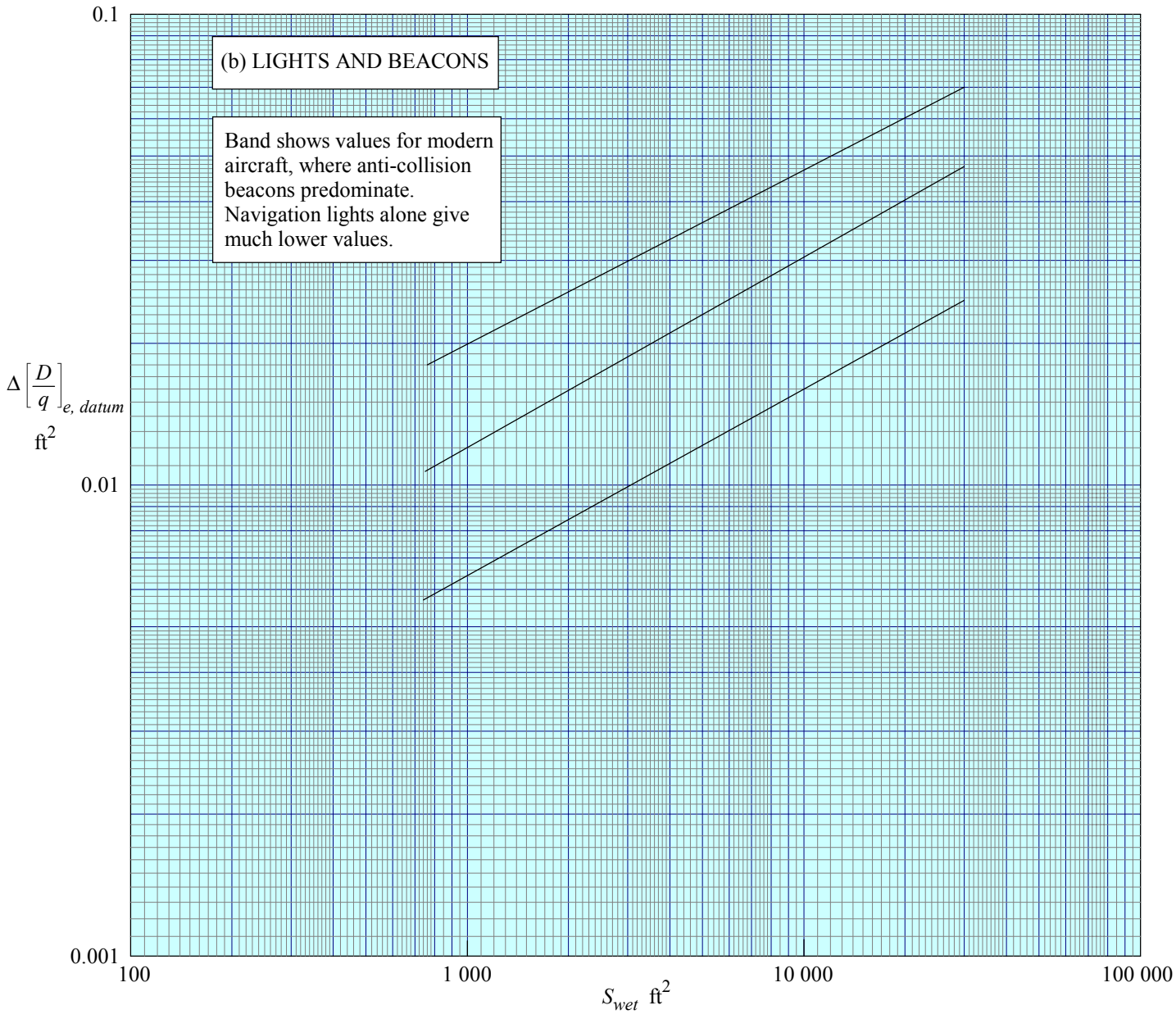

FIGURE 4 EXCRESCENCE DRAG LEVELS DUE TO AIRCRAFT SYSTEMS (AT DATUM CONDITIONS OF H_p AND M)

Class of aircraft	Maximum M in level flight
1. Transports with modern low-drag antennae	0.78 to 0.86
2. Jet transports designed before 1970	0.75 to 0.88
3. Jet combat types	0.7 to 0.9
4. Supersonic types	1.4 to 2
5. High performance propeller-driven combat/trainer types	0.45 to 0.6
6. Old propeller-driven bombers/transports	0.3 to 0.4

(c) ANTENNAE

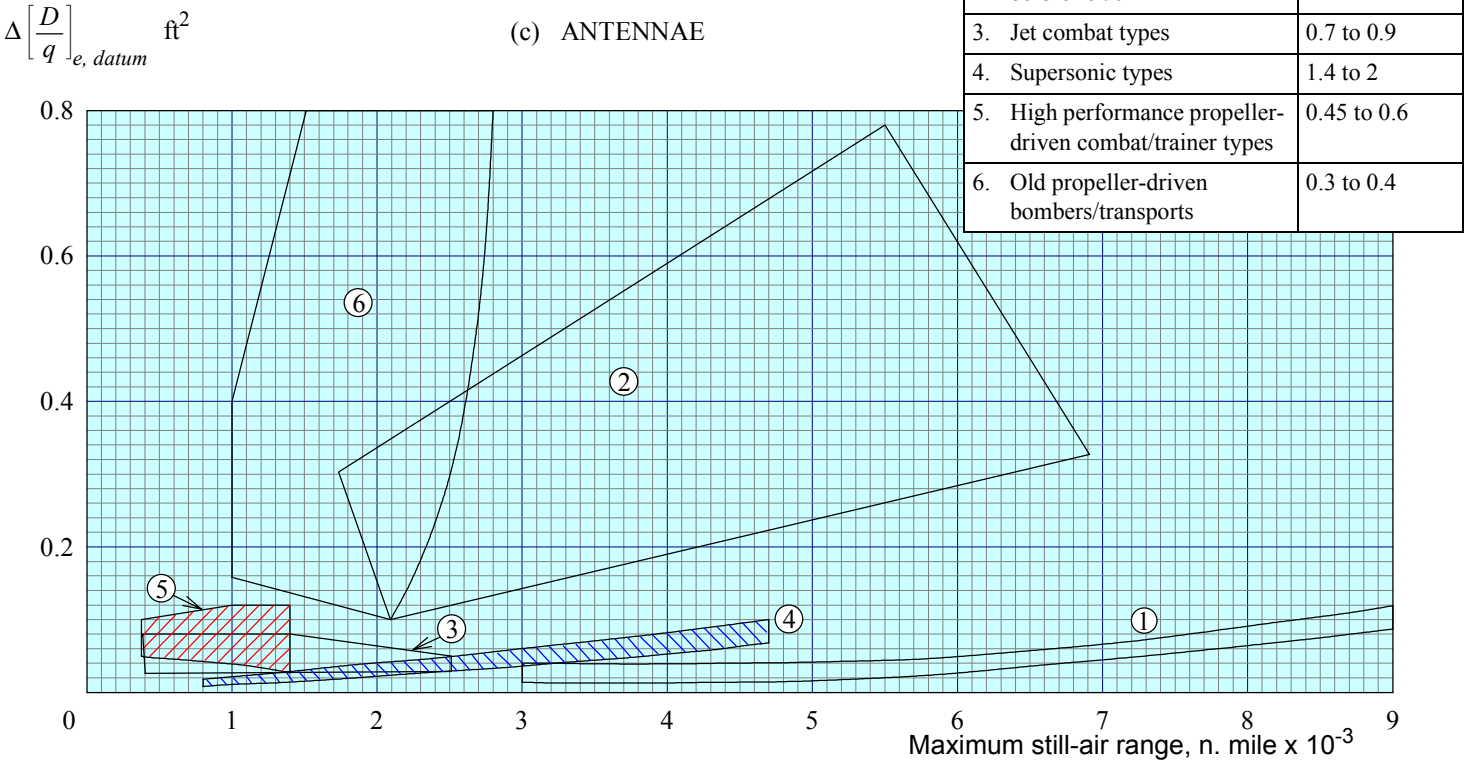

(d) STATIC DISCHARGE WICKS (RIGID TYPES)

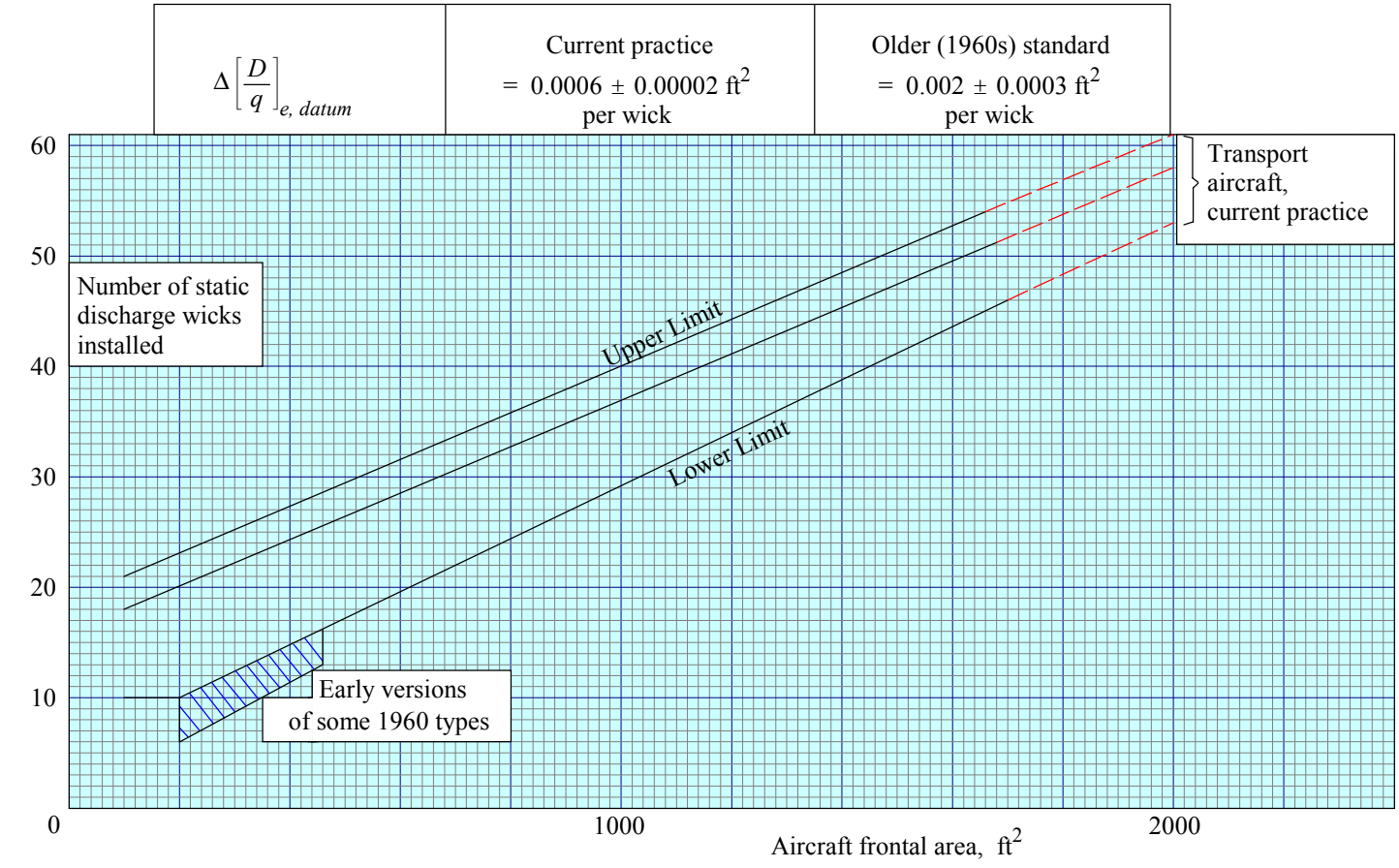

FIGURE 4 (Continued)

(e) RAIN DISPERSAL

Description	$\Delta\left[\frac{D}{q}\right]_{e,\,datum}$ ft^2
Low drag dispersal systems for screens	[width of pilots screen panels] × 0.004
Typical older-style (1960s) screen wipers	[width of pilots screen panels] × 0.02
Highest estimated values for screen wipers	[width of pilots screen panels] × 0.05
Gutters above doors	0.0018 per passenger door

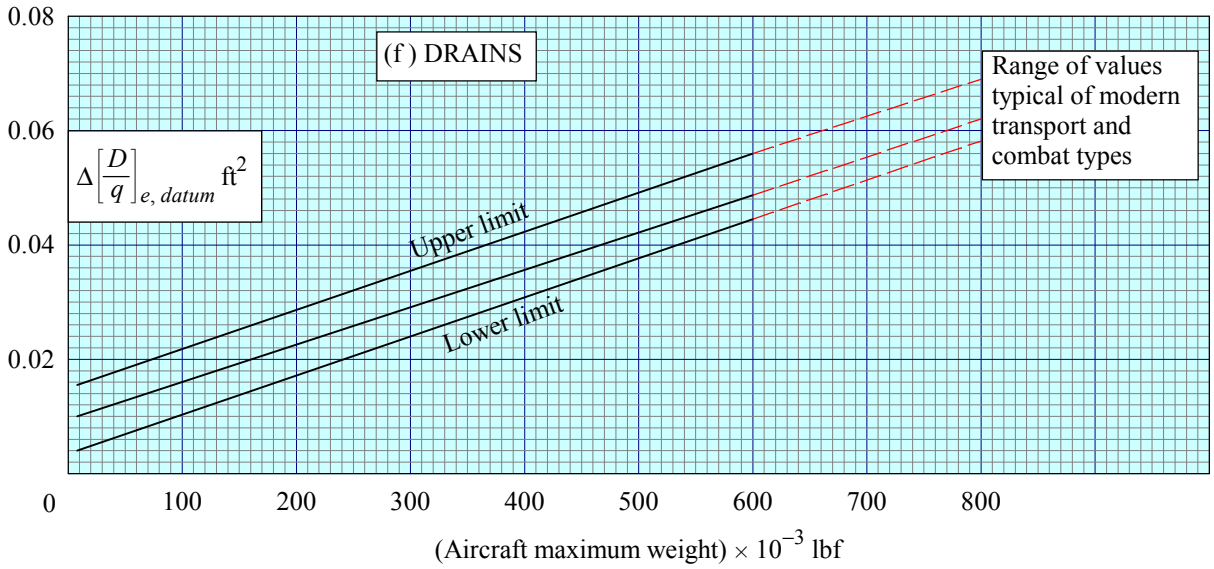

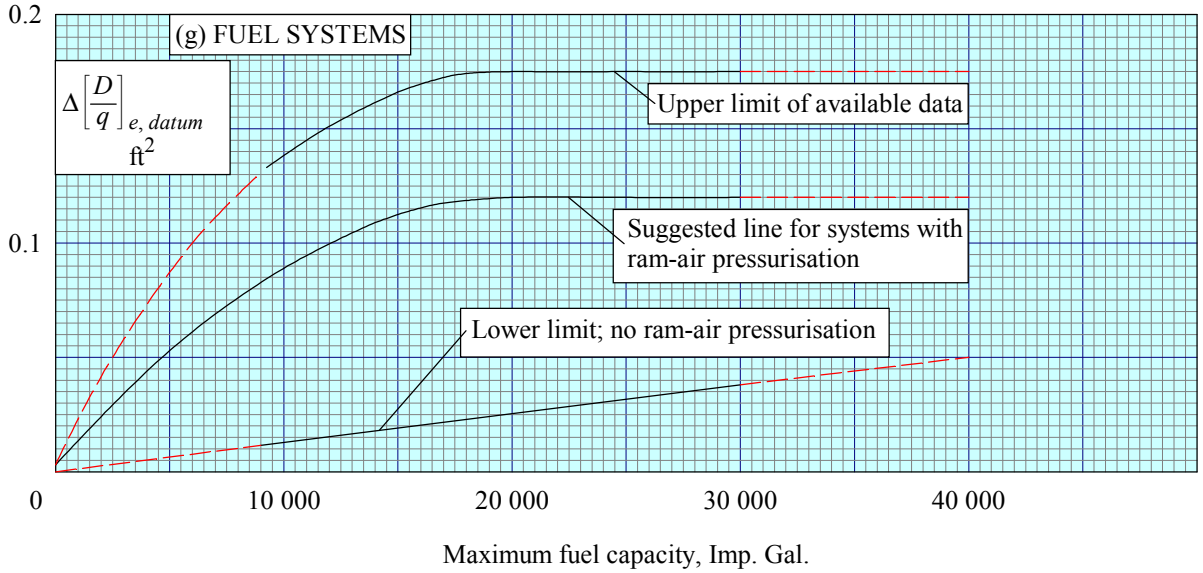

FIGURE 4 (Concluded)

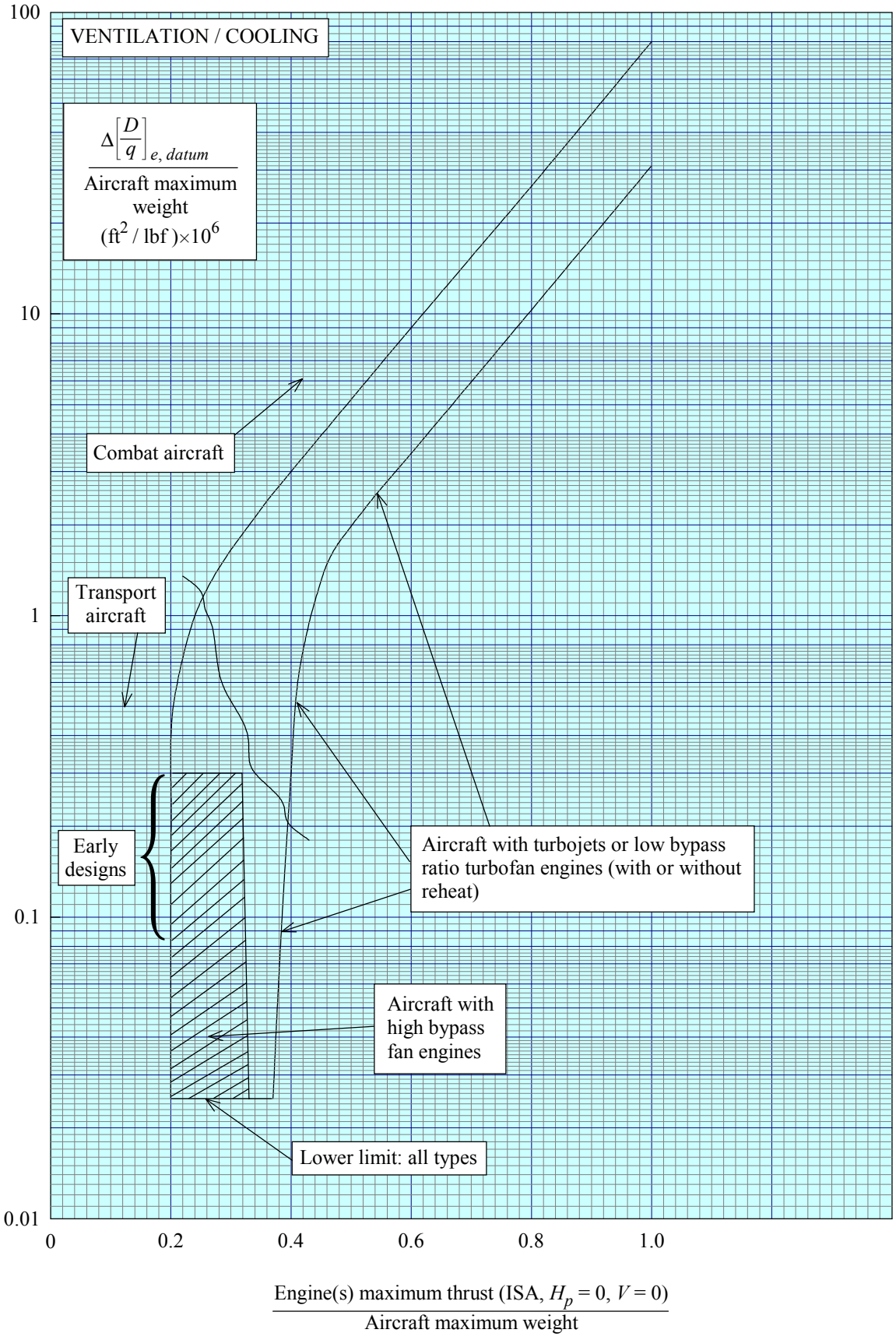

FIGURE 5 EXCRESCENCE DRAG LEVELS DUE TO VENTILATION/COOLING SYSTEMS (AT DATUM CONDITIONS OF H_p AND M)

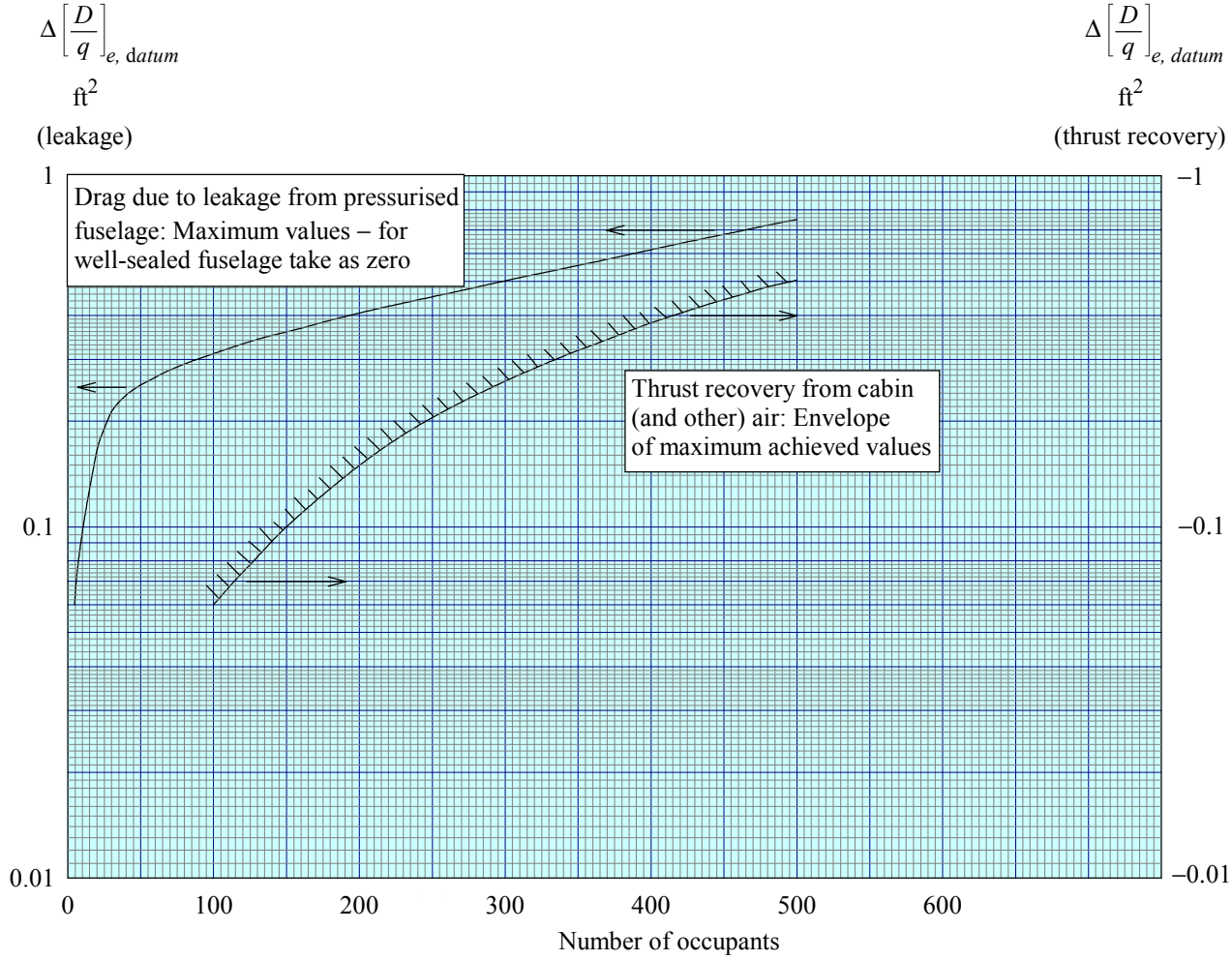

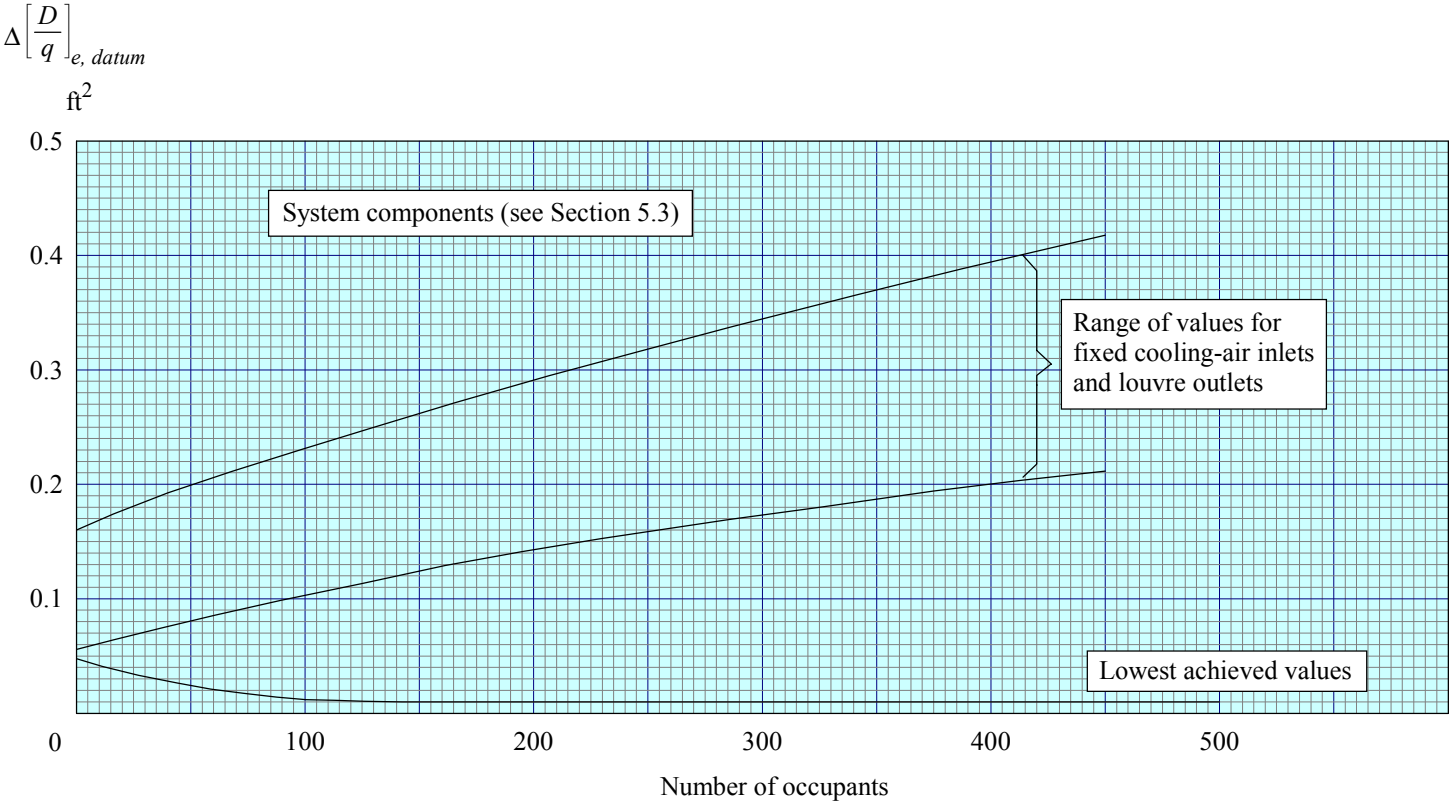

FIGURE 6 EXCRESCENCE DRAG LEVELS DUE TO AIR CONDITIONING SYSTEMS (AT DATUM CONDITIONS OF H_p AND M)

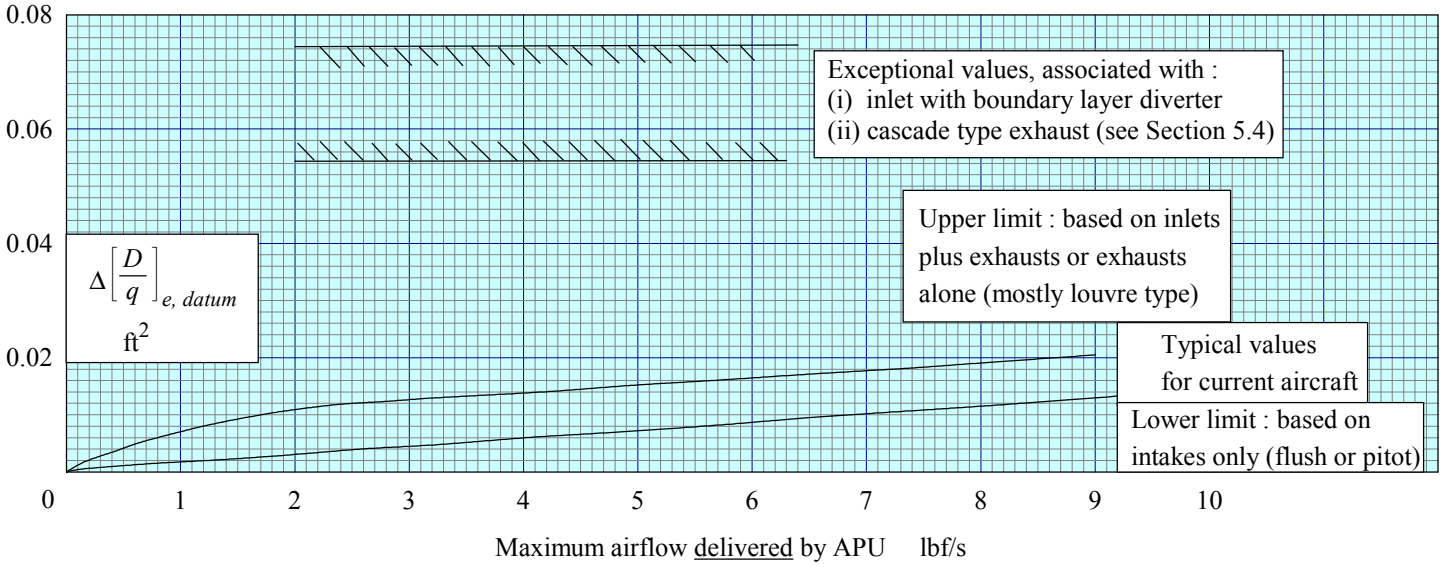

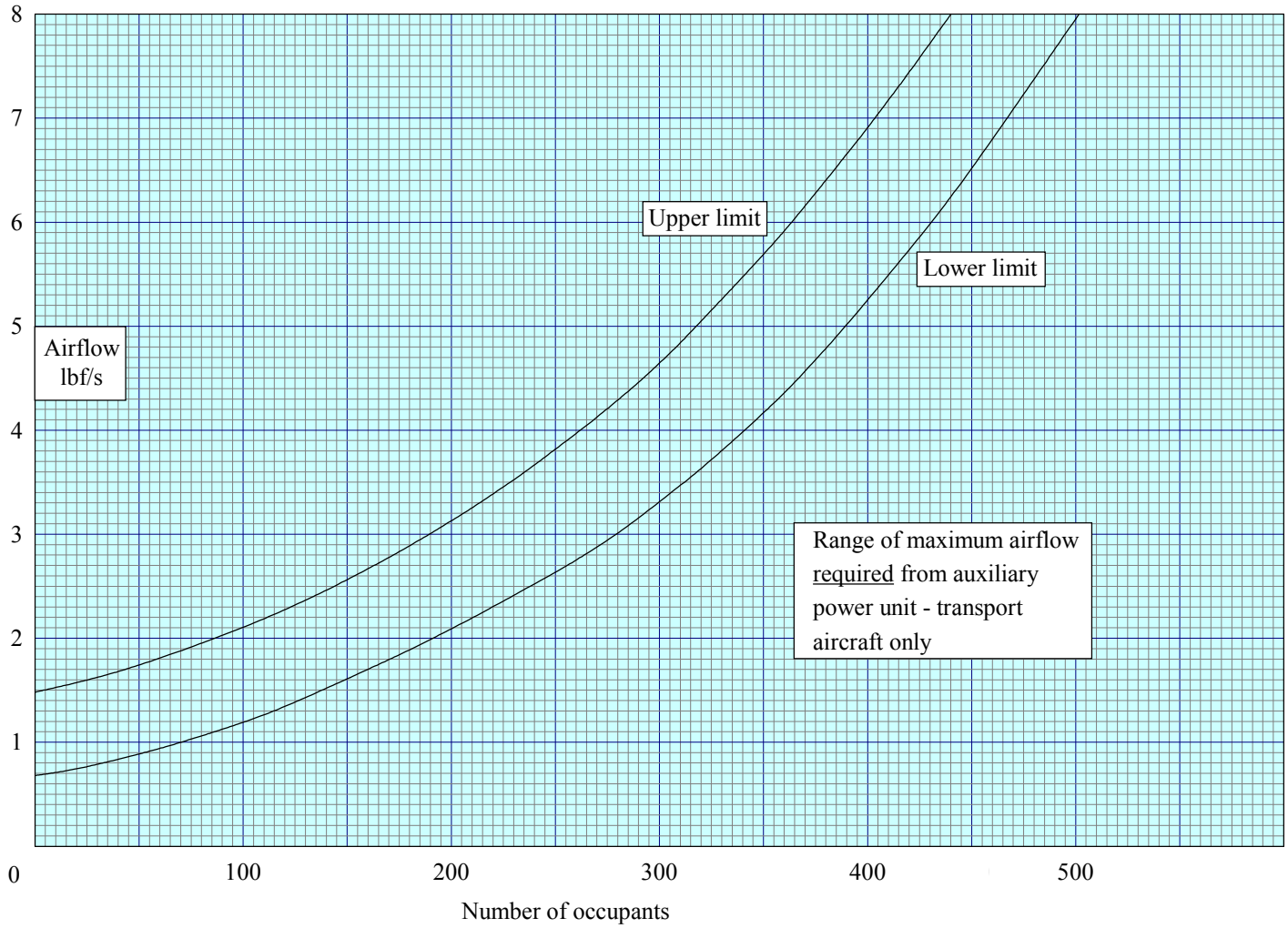

FIGURE 7 EXCRESCENCE DRAG LEVELS DUE TO AUXILIARY POWER UNIT (AT DATUM CONDITIONS OF H_p AND M)

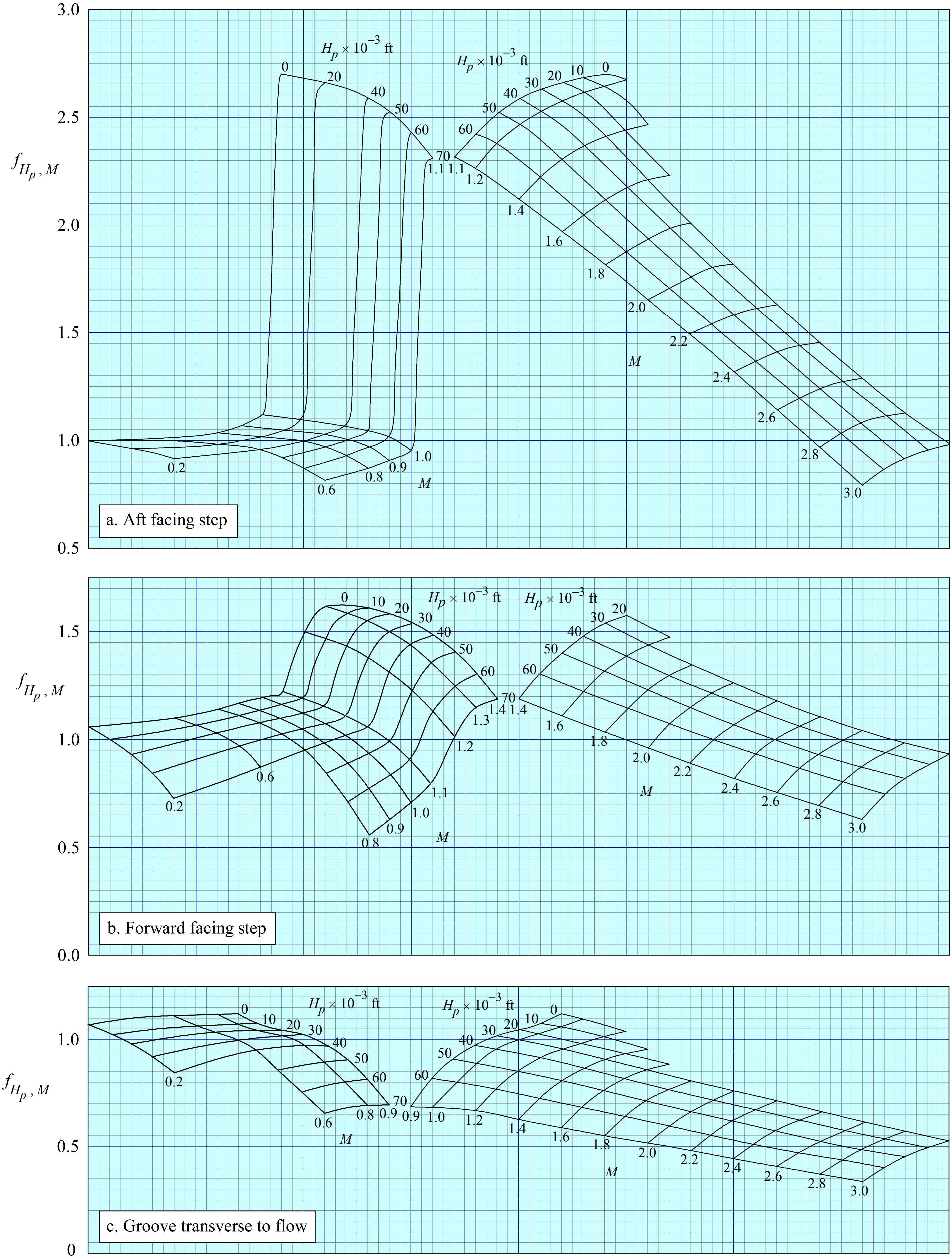

FIGURE 8 EFFECTS OF PRESSURE HEIGHT AND MACH NUMBER ON EXCRESCENCE DRAG

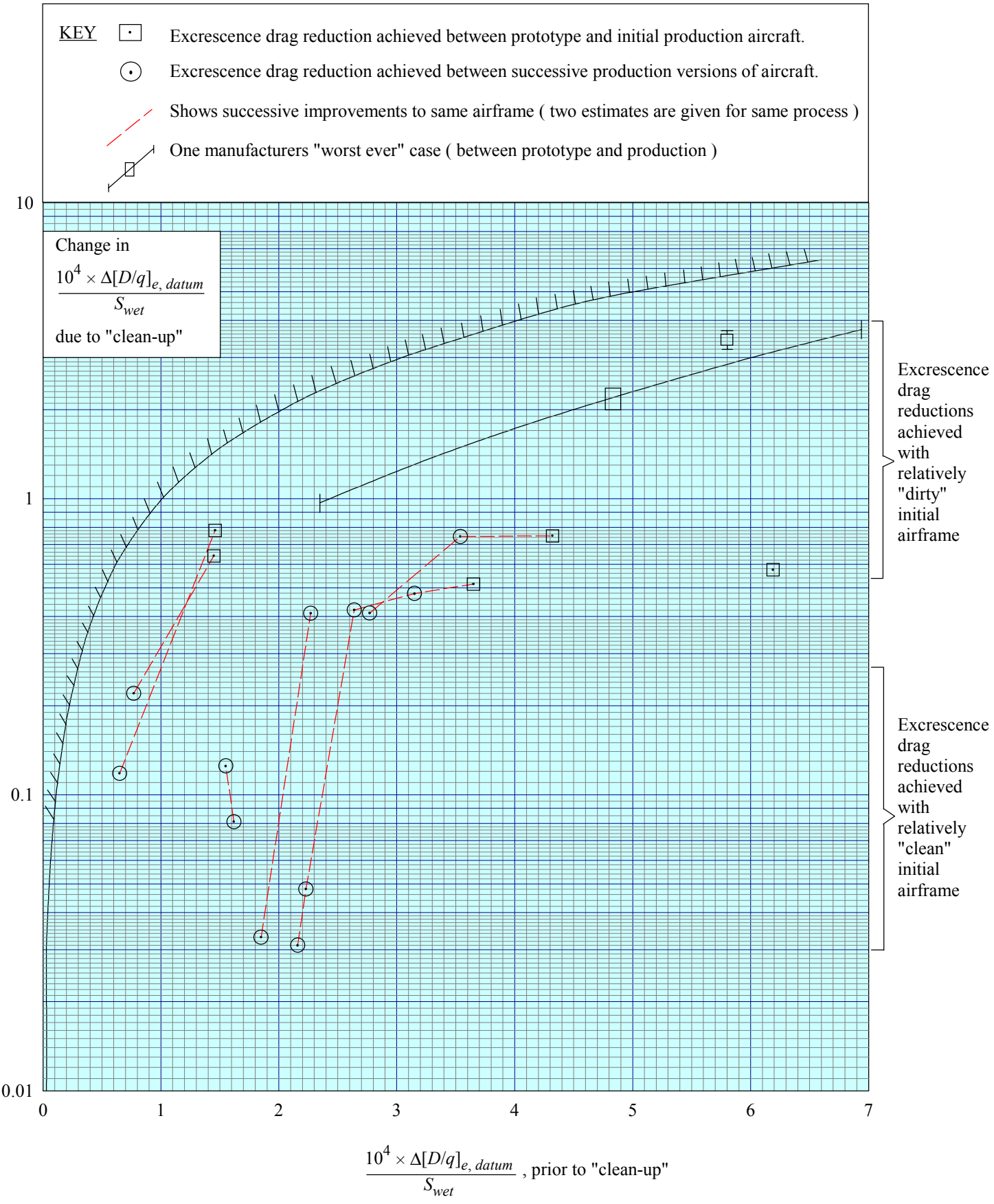

FIGURE 9 EXCRESCENCE DRAG REDUCTION DUE TO AIRFRAME CLEAN-UP

APPENDIX A LIST OF EXCRESCENCES

For a detailed estimate of excrescence drag a systematic scheme is required to account for each excrescence and eliminate duplication. It is also convenient to record the contributions to excrescence drag using several methods of subdivision – the most common of which are as follows.

Location of excrescences: wing, fuselage, tailplane, fin, pylons, nacelles.
Type of excrescences: surface imperfections, steps, ridges, holes, *etc*.
Systems giving rise to excrescences: air data system, fuel system, auxiliary power unit, *etc*.

The need for rigorous accounting is emphasised by these types of subdivision since all excrescences fall into two of the categories and many into all three. The subdivision of excrescences used in Section 5 is repeated below together with cross references to the examples given in this Appendix. The examples are a compilation of all the excrescences identified in the data used in deriving Figures 2 to 7.

Category of excrescence			see Appendix A Section
Basic airframe	1.	Airframe-build surface imperfections.	A1
	2.	Imperfections associated with movable aerodynamic surfaces.	A2
Fixed external components of aircraft systems	3.	Air data sensors.	A3
	4.	Lights and beacons.	A4.
	5.	Antennae.	A5
	6.	Static discharge wicks.	A6
	7.	Rain dispersal: screen wipers/blowing/fluid; gutters over doors.	A7
	8.	Drains.	A8
	9.	Fuel system.	A9
Internal Airflow Systems	10.	Ventilation/cooling.	A10.
	11.	Air conditioning/pressurisation.	A11
	12.	Auxiliary power unit.	A12
	13.	Miscellaneous airframe features.	5.4

A1. AIRFRAME-BUILD SURFACE IMPERFECTIONS

Features common to all airframe parts

skin joints, doublers, steps, gaps, seams
fasteners: (rivets, bolts, screws)
waviness
access panels: grooves, steps, fasteners

Wing

manholes – fuel tank access
access panels: aileron, slat actuators
undercarriage doors; steps, grooves
wing-glove steps, seals (variable geometry)
leading-edge joint
expansion joints
external reinforcing
trailing-edge wrap around

aileron, tab, spoilers: hinges, linkages, actuators, jacks, fairings

jacking point
lifting plug
escape rope bracket
tie down rings
walkway

Flap track fairings

flap linkages
exposed bearings
gear boxes
track closing plates
roller fairings
access panels

Fin and rudder

bullet base
access panels
accelerometer brackets
fin-dorsal junction expansion joint
heat shield
rudder hinge connections, jacks, pins
fairings for hinges and jacks
rudder-wiper-plate seal
access panels

Tailplane/stabiliser/taileron

hinge connections, linkages
fairings for hinges and bearings
wiper plate seal
access panels

Fuselage

nose-radome joints, fasteners, lightning conducter strips
cockpit window joints
windscreen glazing bars
windscreen rain removal access door/hinges
windscreen/canopy fairing
canopy hinge/fuselage spine fairing step
canopy hinges, gaps
canopy handle
droop-nose joint/seal
visor surround
visor glazing
passenger windows; steps, seals
emergency exits seals
airbrakes doors and fairings
crash-recorder access
braking parachute door/fairing
camera access door
vortex generator base
tail bumper
horizontal-tail shield
taileron roller rubbing strips
crash strips
access panels: latches, handles, hinges
wiring ducts

door: passenger, crew, cargo, galley: seals, steps, windows, handles

nose gear, main gear, tail gear, kneeling blisters, bomb bay: seals, steps, fairings on doors

Powerplant

cowl latches
cowl hinged joints
reverser-cowl joints
sliding-cowl break
engine-door gaps, slides
access-panels/fasteners
gloves to pylon or vertical tail gap
engine-mounting fairings
intake/airframe junction
exhaust/airframe junction
nacelle/nozzle joint
nozzle petals
nacelle leakage of high pressure air
wing nacelle seals
pressure and thermal effects on nacelle/doors
auxiliary air intake door, hinges
intake-throat bleed outlets
ground-running airflow doors, hinges

Powerplant pylons

pylon/wing trailing-edge fairing
pylon/slat junction
access panels/fasteners
attachment-lug fairings

A2. IMPERFECTIONS ASSOCIATED WITH MOVABLE AERODYNAMIC SURFACES

Ailerons

leading edge gap/groove
chordwise spacer gap
vent gap
aileron to wing joint

Elevons

seal step at tip
seal step at attachment point
gap between elevons
longitudinal and lateral joints

Slats (upper and lower surfaces)

trailing edge step, groove
inboard end groove
grooves between slat segments
joints between slat segments
slat gaps

Flaps

flap shroud-trailing-edge step/gap/grooves
flap to fixed wing joint
gap/groove between flaps
chordwise grooves at flap ends

Spoilers/airbrakes

leading-edge step/groove
hinge line discontinuity/gap
spoiler to fixed wing joint
spoiler trailing-edge step/gap
spoiler to flap discontinuity
spoiler to spoiler (chordwise) gaps
hinge chordwise gaps/grooves
chordwise grooves at spoiler ends
leakage

Elevator

spanwise gaps
chordwise gaps
stabiliser – elevator leakage

Rudder

spanwise gaps/seals
chordwise gaps/seals
shroud to rudder steps

A3. AIR DATA SENSORS

pitot probe
pitot-static probe
compensated pitot-static probe
total-pressure probe
q-feel pitot probe
nose probe
wing-boom pitot
static tapping
static wedge
static probe
angle-of-attack sensor
sideslip probe
airstream direction detectors
yaw and incidence probe
ball-nose incidence probe
total-temperature probe/sensor
ice detector

A4. LIGHTS AND BEACONS

anti-collision beacon (upper, lower fuselage, tail)
tail logo light
tail/fin trailing-edge light
navigation light
rendezvous/formation light
hook illumination
wing obstruction light
landing light
taxi light

A5. ANTENNAE

Forms of antennae: blade, triangular, dome, rod, wire

Systems

ADF	MADGE	Doppler Decca	TACAN
ALQ XXX	Maker beacon	HF	Transponder
ATC	Radio altimeter	IFF	UHF
DME	Radio compass	ILS marker	VHF

A6. STATIC DISCHARGE WICKS

Locations: wing, winglet, tailplane and fin trailing edge and tip
engine pylons trailing edges

A7. RAIN DISPERSAL

screen wiper arms and blades
screen rain repellent fluid nozzles
screen blowing duct/nozzle
screen washer nozzles
sidescreen washer fairings
gutters over doors

A8. DRAINS (MASTS OR HOLES)

water drains: wing
fuselage
cargo bay
radar bay

fuel drains: engine
reheat pipe
nozzle
A.P.U.
fuel tank bay
refuelling sump

oil drains: gearbox
equipment bay
A.P.U.

hydraulic fluid: brake reservoir
hydraulic system
undercarriage retraction jack

A9. FUEL SYSTEM

fuel-filler cap
fuel overflow
cable fairings to tanks
fuel probe
ram intake for tank pressurisation
fuel jettison pipe/outlet/vent
fuel tank drain valve/outlet

A10. VENTILATION/COOLING

Forms

scoop intake
NACA submerged intake
louvres
holes
step around intakes and exits

Airframe ventilation

Wing

leading edge
forward equipment bay
rear equipment bay
glove (variable geometry)
undercarriage well – tyre/brake cooling

Fuselage

upper fairing/spine
lower fairing
equipment bay
droop nose
radome
cockpit emergency air inlet
engine bay
interspace cooling
engine heat shield
airbrake cavity
tailcone
trim tank

Systems

oil breather
oil cooler
fuel heater exhaust
alternator cooling inlet/outlet
fuel cell vent
storage battery vent
avionics/electronics/radio vent inlets/outlets
hydraulic fluid cooler scoop, vent
oxygen bottle vent
oxygen cylinder rupture discharge port
lavatory waste tank vent
gun gas/gas purge vent
ammunition vent

A11. AIR CONDITIONING/PRESSURISATION

heat-exchanger inlet
ram-air inlet
air-conditioning outlet
cabin-air leakage
cabin-air regulator outflow valves
cockpit exhaust
galley vent
lavatory vent
negative-pressure release vent
thrust recovery nozzle
distortion due to pressurisation
anti-icing air exhaust
primary heat exchanger inlet
primary heat exchanger outlet
secondary heat exchanger inlet
secondary heat exchanger outlet
bleed-air heat exchanger
cover plate over condenser

A12. AUXILIARY POWER UNIT

inlet
inlet and diverter
outlet
fire warning horn

APPENDIX B APPROXIMATE METHOD FOR VARIATION OF EXCRESCENCE DRAG WITH H_p AND M

B1. ADDITIONAL NOTATION

		SI	*British*
A , B	constants in Equation (B3.1)		
C_D	incremental drag coefficient due to a two-dimensional excrescence, based on its height, h, and kinetic pressure at edge of boundary layer		
C_F	mean skin friction coefficient		
C_f	local skin friction coefficient in absence of excrescence, based on kinetic pressure at edge of boundary layer		
F_c	compressibility factor on skin friction, see Equation (B4.10)		
F_δ	compressibility factor on Reynolds number based on momentum thickness, see Equation (B4.11)		
h	height of step or ridge, depth of groove	m	ft
M_δ	Mach number at edge of boundary layer		
Re_h	Reynolds number based on h and on velocity and kinematic viscosity at edge of undisturbed boundary layer ($= \mu_\delta h/\nu_\delta$)		
Re_x	Reynolds number based on x ($= \mu_\delta x/\nu_\delta$)		
Re_{δ_2}	Reynolds number based on δ_2 and velocity and kinematic viscosity at edge of undisturbed boundary layer ($= \mu_\delta \delta_2/\nu_\delta$)		
r	temperature recovery factor		
T	static temperature	K	K
u_δ	velocity at edge of boundary layer	m/s	ft/s
u_τ	friction velocity, $(\tau_\omega/\rho_\omega)^{1/2}$	m/s	ft/s
x	streamwise length from start of turbulent boundary layer	m	ft
γ	ratio of specific heat capacities		
δ	boundary layer thickness	m	ft
δ_2	boundary layer momentum thickness	m	ft
μ	dynamic viscosity	kg/m s	slug/ft s
ν	kinematic viscosity, μ/ρ	m^2/s	ft^2/s
τ_w	wall shear stress	N/m^2	lbf/ft^2
Superscript			
i	denotes equivalent-incompressible, or kinematic, value		
Subscripts			
ω	denotes conditions at wall		
δ	denotes conditions at edge of boundary layer		

B2. INTRODUCTION

This Appendix presents the derivation of values of the factor $f_{Hp,\,M}$ used to provide an approximate method for adjusting the value of $\Delta[D/q]_{e,\,datum}$ obtained from Figures 1 to 7 (applicable to H_p = 36 089 ft (11 000 m) and M = 0.8) to other combinations of H_p and M,

$$f_{Hp,M} = \frac{\Delta[D/q]_e}{\Delta[D/q]_{e,datum}}. \tag{B2.1}$$

The calculations are based on typical variations with Mach and Reynolds numbers of drag data for two-dimensional excrescences (mean height of order 0.1 of the boundary layer height) in conjunction with flat plate turbulent skin friction values and appropriate atmospheric parameters. **Section** B3 describes how the excrescence drag data are represented. **Section** B4. defines the turbulent boundary layer skin friction method used. **Section** B5 describes how the relationships given in Sections B3 and B4. are combined with atmospheric and geometric parameters to deduce the values of $f_{Hp,\,M}$ shown in Figure 8.

B3. ANALYTICAL REPRESENTATION OF MEASURED DRAG DATA FOR TWO-DIMENSIONAL EXCRESCENCES

References 23 and 25 present measured drag data for various two-dimensional excrescences mounted on flat plates and these data, among others, are the basis of References 11, 12 and 24. For excrescence heights which are relatively small compared with the (turbulent) boundary layer height $(h \le 0.1\delta)$, drag data are successfully correlated on the basis of a roughness Reynolds number $(u_\tau h/\nu_w)$ as

$$\frac{C_D}{C_f} = A \log_{10}\left[\frac{u_\tau h}{\nu_w}\right] - B. \tag{B3.1}$$

The constants A and B are dependent on M_δ and the type of excrescence – Figure B1 gives values.

The roughness Reynolds number, $(u_\tau h/\nu_w)$, in Equation (B3.1) can be expressed in the form

$$\frac{u_\tau h}{\nu_w} = \left(\frac{C_f}{2}\right)^{1/2} Re_h \left(\frac{\nu_\delta}{\nu_w}\right)\left(\frac{\rho_\delta}{\rho_w}\right)^{1/2}. \tag{B3.2}$$

The last two terms in Equation (B3.2) can be expressed in terms of static temperatures by using a power law representation for viscosity, taken here as $\mu \propto T^{0.8}$, and assuming that static pressure is constant through the boundary layer, *i.e.* $\rho \propto T^{-1}$. Thus,

$$\left(\frac{\nu_\delta}{\nu_w}\right)\left(\frac{\rho_\delta}{\rho_w}\right)^{1/2} = \left(\frac{\mu_\delta}{\mu_w}\right)\left(\frac{\rho_\delta}{\rho_w}\right)^{-1/2} = \left(\frac{T_\delta}{T_w}\right)^{1.3}. \tag{B3.3}$$

For zero heat transfer, the temperature ratio in Equation (B3.3) can be written as

$$\frac{T_\delta}{T_w} = \left[1 + r\frac{(\gamma - 1)}{2} M_\delta^2\right]^{-1}. \tag{B3.4}$$

With the aid of Equation (B3.4) substitution of Equation (B3.3) into Equation (B3.2) gives

$$\frac{u_\tau h}{\nu_w} = \left(\frac{C_f}{2}\right)^{1/2} Re_h \left[1 + r\frac{(\gamma - 1)}{2} M_\delta^2\right]^{-1.3}. \tag{B3.5}$$

Therefore Equation (B3.1) becomes

$$\frac{C_D}{C_f} = A\log_{10}\left\{\left(\frac{C_f}{2}\right)^{1/2} Re_h \left[1 + r\frac{(\gamma - 1)}{2} M_\delta^2\right]^{-1.3}\right\} - B. \tag{B3.6}$$

For present purposes the values for air of $\gamma = 1.4$ and $r = 0.89$ are used and, for consistency with the skin friction method of Section B4., it is convenient to work in terms of a Reynolds number based on the length, x, of the boundary layer from its origin. Equation (B3.6) then becomes,

$$\frac{C_D}{C_f} = A\log_{10}\left\{\left(\frac{C_f}{2}\right)^{1/2} Re_x \frac{h}{x}[1 + 0.178 M_\delta^2]^{-1.3}\right\} - B. \tag{B3.7}$$

B4. SKIN FRICTION FOR TURBULENT BOUNDARY LAYER ON A FLAT PLATE

The turbulent boundary layer skin friction relationships used here are taken from Reference 25. The Reference provides the most recent detailed experimental evidence together with a comparison with various skin friction laws*. The work in Reference 25 was directed particularly towards the accurate prediction of drag at high (flight) values of Reynolds number.

Within the limitations of the analysis of Reference 25 (primarily the neglect of a sublayer in the velocity profile), the formulae derived therein give a complete description of the mean properties of turbulent boundary layer in zero pressure gradients and with zero heat transfer at Mach numbers below about 5.

Local skin friction coefficient in incompressible flow, C_f^i

(i) Reynolds number based on boundary layer momentum thickness

$$Re_{\delta 2}^{\,i} = 0.3894\left(1 - 4.632(C_f^i)^{1/2}\right)\exp\left[0.537(C_f^i)^{-1/2}\right]. \qquad \text{(B4.1)}$$

An interpolation formula† giving C_f^i within 0.04% of the values given by Equation (B4.1), for $5\times10^3 \le Re_{\delta_2}{}^i \le 5\times10^5$, is

$$C_f^i = \frac{0.01013}{\log_{10} Re_{\delta 2}^{\,i} - 1.02} - 0.00075\,. \qquad \text{(B4.2)}$$

(ii) Reynolds number based on streamwise length from start of boundary layer

$$C_f^i Re_x^{\,i} = 0.7788\left[1 - 8.353(C_f^i)^{1/2} + 24.16(C_f^i)\right]\exp\left[0.537(C_f^i)^{-1/2}\right]. \qquad \text{(B4.3)}$$

An interpolation formula† giving C_f^i within 0.5% of the values given by Equation (B4.3), for $5\times10^5 \le Re_x \le 10^9$, is

---

* **Extracts from Reference 25, Section 6.4:**

"Comparison with some Current Methods of Estimating Turbulent Skin Friction

In general the available methods for estimating turbulent skin friction are of a semi-empirical nature and, because of the lack of measurements at high Reynolds numbers, might be expected to be most reliable at Reynolds number up to say 10 million. One purpose of the present experiment was to assess (as far as is possible with one set of measurements which may contain systematic errors) the applicability of these methods at high Reynolds number." .....

"Further comparisons with the predictions of Sommer and Short[27], Spalding and Chi[29] and Coles[28] are given ..... The comparisons are made for the variations of local skin-friction coefficient with Reynolds number based on momentum thickness, both parameters being reduced to incompressible form by the compressibility factors appropriate to each method. Of the three methods, that of Sommer and Short clearly fits best the present data. The method utilises the Karman-Schoenherr relationship for incompressible flow, which is very close to that derived from the present experiments, and this is in fair agreement with the results at $M_\delta = 0.2$. The compressibility factors are also apparently satisfactory, though there is perhaps a tendency for skin friction to be underestimated at $M_\delta = 1.4$ and 2.2 at the upper end of the Reynolds number range. The other two methods also give good predictions of the low speed data. The method of Spalding and Chi overestimates the skin friction at supersonic speed particularly at lower Reynolds number, whereas the method of Coles underestimates particularly at higher Reynolds number. On the evidence of the present data both these methods would therefore have a common failing in predicting too great a reduction in drag in extrapolating from wind tunnel tests at low Reynolds number and supersonic speed to the Reynolds numbers for full scale aircraft".

† Equation (B4.2) is presented in Reference 23 while Equation (B4.4) was derived in analagous fashion in Reference 24.

$$C_f^i = \frac{0.01224}{\log_{10} Re_x^i - 3.209} - 0.00075 . \quad \text{(B4.4)}$$

Mean skin friction coefficient in incompressible flow, C_F^i

$$C_F^i Re_x^i = 0.7788\left[1 - 4.632(C_f^i)^{1/2}\right]\exp\left[0.537(C_f^i)^{-1/2}\right]. \quad \text{(B4.5)}$$

Compressibility factors and relationships

$$C_f^i = F_c C_f, \quad \text{(B4.6)}$$

$$C_F^i = F_c C_F, \quad \text{(B4.7)}$$

$$Re_{\delta_2}^i = F_\delta Re_{\delta_2}, \quad \text{(B4.8)}$$

$$Re_x^i = \frac{F_\delta}{F_c} Re_x, \quad \text{(B4.9)}$$

$$F_c = (1 + 0.2M_\delta^2)^{1/2}, \quad \text{(B4.10)}$$

$$F_\delta = 1 + 0.056M_\delta^2. \quad \text{(B4.11)}$$

B5. CALCULATION PROCEDURE FOR FACTOR $f_{Hp,\,M}$

This Section outlines the procedure used to calculate the values of $f_{Hp,\,M}$ from which Figure 8 has been derived. The factor $f_{Hp,\,M}$ is defined by the relationship

$$f_{Hp,\,M} = \frac{\Delta[D/q]_e}{\Delta[D/q]_{e,datum}} \quad \text{(B5.1)}$$

and the aim of the following calculation procedure (steps (i) to (vii)) is to deduce values* $\Delta[D/q]_e$ in terms of excrescence geometry, *i. e.* A, B, h, x; Mach number, with $M_\delta = M$; and pressure height H_p.

(i) **Definition**: the excrescence drag parameter* $\Delta[D/q]_e$ is related to C_D/C_f (see Equation (B3.7)) by

$$\Delta\left[\frac{D}{q}\right]_e = \left[\frac{C_D}{C_f}\right] \times C_f \times h . \quad \text{(B5.2)}$$

(ii) **Excrescence drag representation:** Equation (B3.7) requires values of the constants A and B and these are given in Figure B1 for three types of two-dimensional excrescence.

* The procedure for obtaining the datum value $\Delta[D/q]_{e,\,datum}$ is similar to that for $\Delta[D/q]_e$ but is simplified by its restriction to the datum conditions $M = 0.8$, $H_p = 36\,089$ ft (11 000 m).

(iii) **Excrescence geometry and location:** The calculations require values of h and x; the following values have been used.

x	m ft	0.152 0.5	3.05 10	15.24 50	
h	mm ft	0.3 0.001	1 0.0033	1.52 0.005	3.04 0.01

(iv) **Local skin friction**: Values of C_f for use in Equation (B3.7) are obtained from the combined use of Equation (B4.3) (or (B4.4)) with Equations (B4.6), (B4.9), (B4.10) and (B4.11).

(v) **Reynolds number**: The value of Re_x for use in Equation (B4.9) is obtained (by definition and the assumption that freestream conditions apply at the edge of the boundary layer) as

$$Re_x = \frac{u_\delta x}{\nu_\delta} = \frac{Ma\rho_\delta x}{\mu_\delta}. \qquad \text{(B5.3)}$$

(vi) **Atmospheric properties**: Values of speed of sound, a, air density, ρ, and dynamic viscosity, μ, for use in Equation (B5.3) are calculated using the relationships given in Data Item No. 77022 (Reference 6). From Section 6 of that Reference, a and ρ are functions of temperature, T, only while Table 11.3 of Reference 6 gives relationships between T, ρ and H_p for the International Standard Atmosphere and for associated "off-standard atmospheres". Consequently, values of a, ρ, μ can be obtained,

either, for ISA conditions, as a function of H_p only,

or, for off-ISA conditions, as a function of H_p and ΔT_{H_p}, where ΔT_{H_p} is a temperature increment applied at all values of H_p to create the off-standard atmosphere.

(vii) **Results:** Sketch B5.1 shows examples of calculated values of $f_{H_p,\,M}$ for an aft-facing step. Similar calculations were performed for all values of x, h listed in (iii), above, for all the excrescence characteristics shown in Figure B1.

Mean lines were drawn through the results and used as the basis of Figure 8. In assessing where to place those mean lines, the following limitations were imposed.

The minimum excrescence height was taken as h = 1 mm (0.0033 ft).

The combination of h = 3 mm (0.01 ft) with x = 0.152 m (0.5 ft) was ignored as being improbable from both the practical viewpoint and as a case where h could be of order 0.1δ.

Combinations of H_p and M corresponding to equivalent airspeeds greater than 800 knots equivalent airspeed were ignored.

At M = 0.2, values were considered only up to H_p = 20 000 ft.

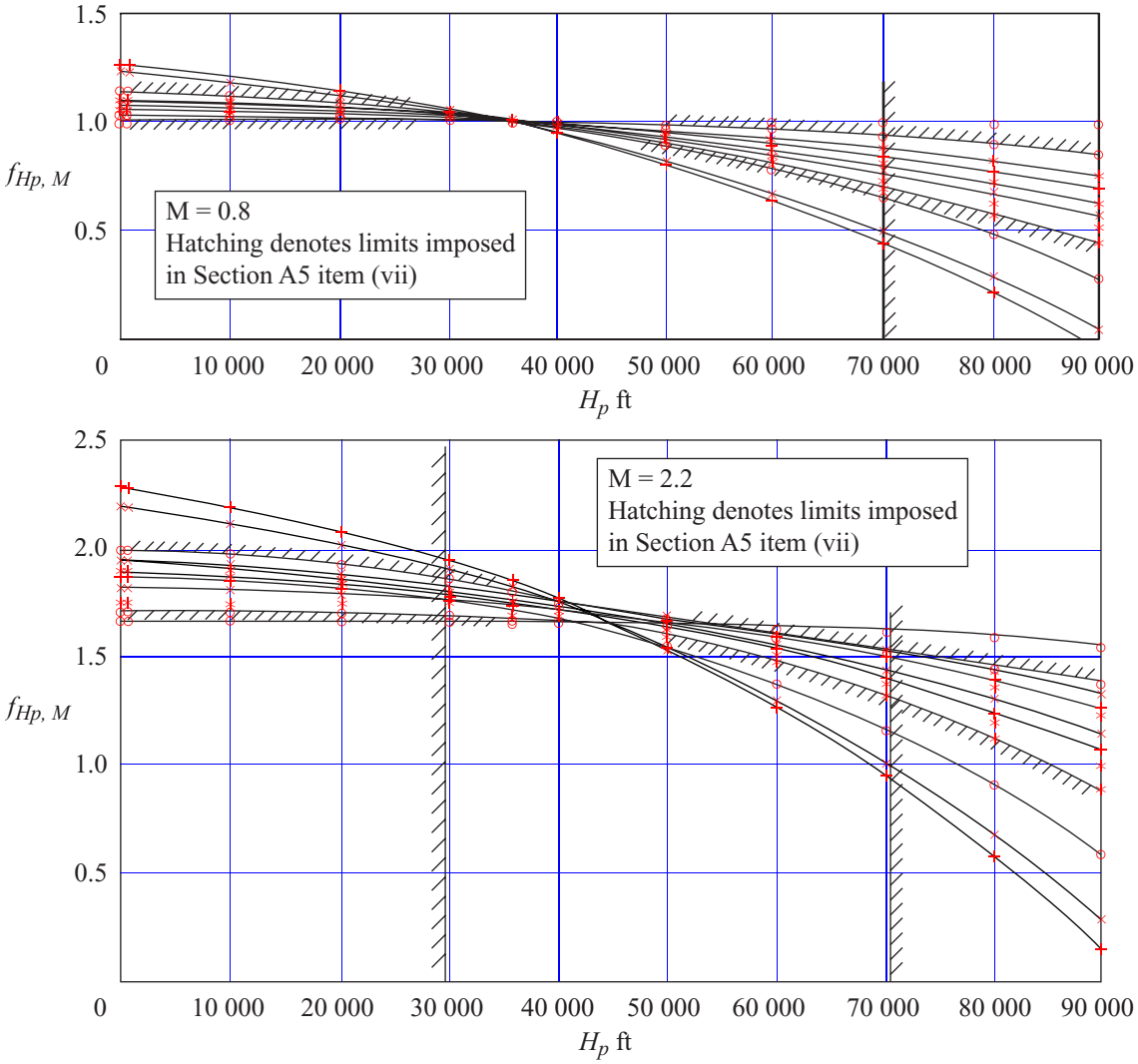

Sketch B5.1 Examples of calculated values of $f_{H_p,\,M}$ for aft-facing step

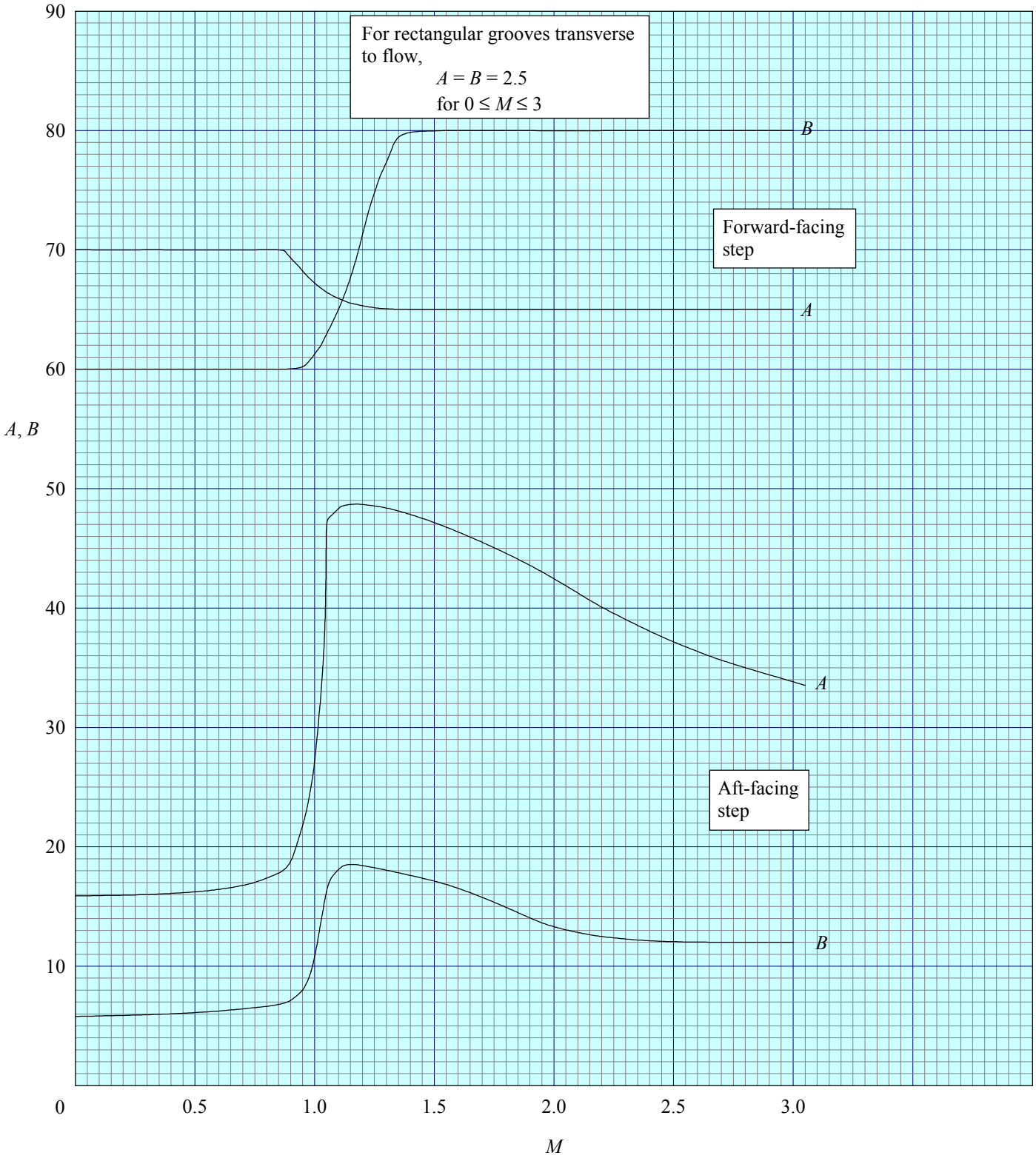

FIGURE B1 VALUES OF CONSTANTS *A* AND *B* IN EMPIRICAL REPRESENTATION OF EXCRESCENCE DRAG (EQUATION (B3.1))

THE PREPARATION OF THIS DATA ITEM

The work on this particular Data Item was monitored and guided by the Performance Committee, which first met in 1946 and now has the following membership:

Chairman
Mr K.J. Balkwill – Independent

Vice-Chairman
Mr W.L. Horsley – Civil Aviation Authority, Safety Regulation Group

Members
Mr T. Bartup – Avro International Aerospace, Woodford
Mr T.B.A. Boughton – Independent
Mr J. Bradley – Aeroplane and Armament Evaluation Establishment
Mr E.N. Brailsford – Independent
Mr M. Broad – Independent
Mr P.D. Feig* – General Electric Company, Cincinnati, Ohio, USA
Mr N.J. Herniman – Airbus Industrie, Toulouse, France
Mr R.G. Humpston – Rolls-Royce Ltd, Derby Engine Division
Dr L.R. Jenkinson – Loughborough University of Technology
Mr T.S.R. Jordan – Independent
Mr W.T. Lewerenz* – McDonnell Douglas, Long Beach, Calif., USA
Mr A.N. Page – Raytheon Corporate Jets Inc., Hatfield
Mr P. Robinson – Independent
Mr R.C. Shields* – Boeing Commercial Airplane Company, Seattle, Wash., USA
Mr D.N. Sinton – Shorts, Belfast
Mr G.J.R. Skillen – Civil Aviation Authority, Safety Regulation Group
Mr G.E. Smith – Independent
Mr A. Stanbrook – Independent
Mr R. Storey – British Aerospace Defence Ltd, Brough
Prof. E. Torenbeek* – Delft University of Technology, Holland
Mr Y.D. Traeger* – Grumman Aircraft Systems, Bethpage, NY, USA.

* Corresponding Member

The technical work involved in the assessment of the available information and the construction and subsequent development of the Data Item was carried out by

Mr D.J. Mitchell.

The person with overall responsibility for the work in this subject area is Mr D.J. Mitchell.